COMPUTATIONAL STUDIES OF EVAPORATING SPRAYS IN A SHEAR LAYER

FINAL REPORT

Bakhtier Farouk

October 1988

U. S. Army Research Office

Contract number DAAL03-87-K-0015

Department of Mechanical Engineering and Mechanics
Drexel University
Philadelphia, PA 19104

Approved For Public Release;
Distribution Unlimited.

UNCLASSIFIED
SECURITY CLASSIFICATION OF THIS PAGE

MASTER COPY

FOR REPRODUCTION PURPOSES

REPORT DOCUMENTATION PAGE

1a. REPORT SECURITY CLASSIFICATION Unclassified	1b. RESTRICTIVE MARKINGS
2a. SECURITY CLASSIFICATION AUTHORITY NA	3. DISTRIBUTION / AVAILABILITY OF REPORT Approved for public release; distribution unlimited.
2b. DECLASSIFICATION / DOWNGRADING SCHEDULE NA	
4. PERFORMING ORGANIZATION REPORT NUMBER(S) NA	5. MONITORING ORGANIZATION REPORT NUMBER(S)
6a. NAME OF PERFORMING ORGANIZATION Drexel University 6b. OFFICE SYMBOL (If applicable) NA	7a. NAME OF MONITORING ORGANIZATION U. S. Army Research Office
6c. ADDRESS (City, State, and ZIP Code) 32nd and Chestnut Streets Philadelphia, PA 19104	7b. ADDRESS (City, State, and ZIP Code) P. O. Box 12211 Research Triangle Park, NC 27709-2211
8a. NAME OF FUNDING / SPONSORING ORGANIZATION U. S. Army Research Office 8b. OFFICE SYMBOL (If applicable)	9 PROCUREMENT INSTRUMENT IDENTIFICATION NUMBER
8c. ADDRESS (City, State, and ZIP Code) P. O. Box 12211 Research Triangle Park, NC 27709-2211	10. SOURCE OF FUNDING NUMBERS PROGRAM ELEMENT NO / PROJECT NO. / TASK NO. / WORK UNIT ACCESSION NO.

11 TITLE (Include Security Classification)
Computational studies of Evaporating Sprays in a Shear Layer

12 PERSONAL AUTHOR(S)
Bakhtier Farouk

13a. TYPE OF REPORT	13b. TIME COVERED	14. DATE OF REPORT (Year, Month, Day)	15. PAGE COUNT
FINAL	FROM 1/14/87 TO 5/14/88	1988/10/21	79

16 SUPPLEMENTARY NOTATION
The view, opinions and/or findings contained in this report are those of the author(s) and should not be construed as an official Department of the Army position, policy, or decision, unless so designated by other documentation.

17 COSATI CODES		
FIELD	GROUP	SUB-GROUP

18. SUBJECT TERMS (Continue on reverse if necessary and identify by block number)
Spray evaporation, turbulent shear layers, computational methods.

19 ABSTRACT (Continue on reverse if necessary and identify by block number)

The objective of the research project was to numerically predict the characteristics of evaporating sprays in a turbulent shear layer. The calculations were performed such that the essential physical processes in spray evaporation in gas turbine combustors are adequately realized The calculations modeled parallel experiments (ARO Contract number DAAG29-84-K-0165) carried out in a vertically down-flowing wind tunnel where a splitter plate separates two air streams having different velocities. The two air streams meet at the end of the splitter plate and give rise to a confined shear layer. A flat prefilming airblast atomizer is located at the tip of the splitter plate. A liquid spray formed at the atomizer tip evaporates in the turbulent shear layer and is convected downstream.

An Eulerian description of the turbulent gas phase flow and a Lagrangian formulation of the droplet size class motion and heat and mass transfer were considered. Single phase two dimensional turbulent flow calculations in a duct were considered. A parabolic formulation of the governing equations along with a k-ε turbulent model was used to obtain the

20 DISTRIBUTION / AVAILABILITY OF ABSTRACT ☐ UNCLASSIFIED/UNLIMITED ☐ SAME AS RPT. ☐ DTIC USERS	21. ABSTRACT SECURITY CLASSIFICATION Unclassified
22a. NAME OF RESPONSIBLE INDIVIDUAL	22b. TELEPHONE (Include Area Code) / 22c. OFFICE SYMBOL

DD FORM 1473, 84 MAR

83 APR edition may be used until exhausted.
All other editions are obsolete.

SECURITY CLASSIFICATION OF THIS PAGE
UNCLASSIFIED

computed flow fields. The values of turbulent mixing time within the shear layer were computed and compared with those predicted by the characteristic time model. For droplets injected into the turbulent air stream, a deterministic separated model was utilized for calculating their trajectories, temperatures and evaporation rates. Typically, a Rossin-Rammler size distribution function was employed for the droplets at the inlet. Solutions were obtained for both water and Jet-A fuel at the liquid phase. The calculated SMD (Sauter mean diameter) variations along the tunnel axis compared favorably with the measurements. To account for the turbulent dispersion of the droplets due to the gas phase turbulence, a stochastic separated flow model was developed. In particular, the spread rate of the spray due to the dispersion effects were evaluated.

ABSTRACT

The objective of the research project was to numerically predict the characteristics of evaporating sprays in a turbulent shear layer. The calculations were performed such that the essential physical processes in spray evaporation in gas turbine combustors are adequately realized. The calculations modeled parallel experiments (ARO Contract number DAAG29-84-K-0165) carried out in a vertically down-flowing wind tunnel where a splitter plate separates two air streams having different velocities. The two air streams meet at the end of the splitter plate and give rise to a confined shear layer. A flat prefilming airblast atomizer is located at the tip of the splitter plate. A liquid spray formed at the atomizer tip evaporates in the turbulent shear layer and is convected downstream.

An Eulerian description of the turbulent gas phase flow and a Lagrangian formulation of the droplet motion and heat and mass transfer were considered. Single phase two dimensional turbulent flow calculations in a duct were considered. A parabolic formulation of the governing equations along with a k-ϵ turbulence model was used to obtain the computed flow fields. The values of turbulent mixing time within the shear layer were computed and compared with those predicted by the characteristic time model. For droplets injected into the turbulent air stream, a deterministic separated model was utilized for calculating their trajectories, temperatures and evaporation rates. Typically, a Rosin-Rammler size distribution function was employed for the droplets at the inlet. Solutions were obtained for both water and Jet-A fuel as the liquid phase. The calculated SMD (Sauter mean diameter) variations along the tunnel axis compared favorably with the measurements. To account for the turbulent dispersion of the droplets due to the gas phase turbulence, a stochastic separated flow model was developed. In particular, the spread rate of the spray due to the dispersion effects were evaluated.

TABLE OF CONTENTS

		Page
	Abstract	3
	Table of Contents	4
	Acknowledgements	6
	Nomenclature	7
I.	INTRODUCTION AND BACKGROUND	9
II.	ANALYSIS OF TURBULENT SHEAR FLOW IN A DUCT	
	II.1. General approach	13
	II.2. Turbulence model	14
	II.3. Initial and boundary conditions for the mean flow quantities	15
	II.4. Initial and boundary conditions for the turbulent flow quantities	17
	II.5. Numerical Methods	20
	II.6 Results and discussion	21
III.	ANALYSIS OF DROPLET BEHAVIOR - DETERMINISTIC MODEL	
	III.1 General approach	43
	III.2 Momentum equations	44
	III.3 Heat and mass transfer equations for droplets	45
	III.4 Droplet class and distribution functions	53
	III.5 Numerical Methods	54
	III.6 Results and discussion	55
IV.	ANALYSIS OF DROPLET BEHAVIOR - STOCHASTIC MODEL	
	IV.1 Background and general approach	60
	IV.2 Mathematical model	63
	IV.3 Modifications to the PTRAK code	64
	IV.4 Results and discussion	68
V.	SUMMARY AND CONCLUSIONS	73

VI. REFERENCES..... 75

APPENDICES

1. List of all publications under sponsorship of ARO
2. List of all participating scientific personnel

Acknowledgements

The author wishes to thank Professor A. M. Mellor for providing the initial thoughts and encouragements to carry out the research performed. Thanks also go to Mr. K. V. Tallio for his interest in the work . A special note of thanks to Messrs. W. Lau and X. X. Cai for devoting many hours on this project.

The support of the Army Research Office, and in particular the assistance provided by Dr. David M. Mann as Technical Monitor is appreciated.

NOMENCLATURE

C_d	Drag coefficient for the droplets
C_p	Specific heat
C_μ	Empirical constant for the turbulence model
d	Droplet diameter
D	Duct width
e	rate of strain
h	Droplet heat transfer coefficient
k	Turbulent kinetic energy
$\tilde{k}$	Mass transfer coefficient
K	Thermal conductivity
L_e	Turbulent length scale, characteristic length
ℓ	mixing length
M	Molecular weight
p	Pressure
Pr	Prandtl number
$\mathring{q}$	Droplet heat transfer
R	Universal gas constant
Re	Reynolds number
SMD	Sauter mean diameter
Sc	Schmidt number
T	Temperature
t	Time
U	Mean axial velocity
V	Mean normal velocity
u'	Fluctuating (axial) velocity
v'	Fluctuating (normal) velocity
$\mathring{w}$	Droplet evaporation rate
x	Axial coordinate
y	Normal coordinate
Y	Fuel vapor concentration (mole fraction)

Greek letters

δ	Boundary layer thickness
ε	Dissipation rate of turbulence
λ	Shear layer strength, heat of vaporization of fuel
ρ	Density
τ	Shear stress, relaxation time
σ	Standard deviation
μ	Viscosity
Ω	Fuel flow rate
Γ_m	Mass diffusivity of fuel vapor

Subscripts

a	Air
d	Droplet
f	Fuel
l	Liquid phase
s	Surface
w	Wall conditions

I. INTRODUCTION AND BACKGROUND

An experimental research program was initiated at Drexel University under ARO sponsorship (Grant Number DAAG29-84-K-0165) for continuing validation of the characteristic time model [Mellor, 1980]. The characteristic time model is a simplified view of combustion where each of the physical processes which occurs during combustion is considered and a physical time which corresponds to that is computed. The semi-empirical characteristic time models were developed under TARADCOM/ARO/MERADCOM sponsorship for prediction of the effects of fuel properties, combustor inlet conditions and liner geometry on performance of gas turbine engines. Models are available for the correlation and prediction of combustion efficiency, gaseous emissions, lean flame stabilization and ignitability (cold start and altitude relight) in terms of characteristic times thought to describe the fluid mechanics, chemistry and fuel droplet evaporation. By analyzing data from helicopter and aircraft engines it was possible to generate performance curves using the characteristic time model which appear to be 'universal', that is independent of engine and fuel type. This is believed to occur because all conventional turbine combustors utilize turbulent spray diffusion flames for their heat release. At ignition, the lean blowoff limit and other low power operating conditions, fuel evaporation also becomes important. For evaporating sprays in a turbulent shear layer, the only significant characteristic times are τ_{sl} (the residence time in the shear layer) and τ_{eb} (the droplet evaporation time).

In the above program (Grant Number DAAG29-84-K-0165), specially designed laboratory tests were performed in which the turbulent mixing processes were examined in detail for comparison with these models. The objectives were primarily to explore the characteristic time model developed for gas turbine combustors.The fuel evaporation and turbulent mixing times where the emphasis of the program where each could be varied independently in fundamental experiments. A vertical down-flowing wind tunnel (see Figure 1) with a square test section and provisions for laser optics (for droplet size measurements by the forward diffraction technique and evaporation measurements by the absorption technique) and hot wire/film probe insertion were designed and constructed for local measurements of τ_{sl} and τ_{eb}. Presence of a splitter plate which terminates in a flat prefilming airblast atomizer produced a shear layer and fuel spray within the tunnel .The situation in the outer primary zone region of a conventional gas turbine combustor thus could be closely approximated in the test section.

The experimental configuration selected, unlike combustors, is two dimensional (as

shown by measurements), provides optical access, easy probe (hot wire/film) access, a liquid spray injected into a shear layer and a region of primary zone combustor flow that is important to many aspects of its performance. Further, the measurements are related to fundamental interactions between turbulent mixing and liquid evaporation (without combustion) in a clean flow which can be analyzed in an orderly fashion without all of the complexities of practical hardware. The cross-sectional dimensions of the tunnel are 7.65 cm by 7.65 cm, chosen to provide test section mean velocities ranging from 50 to 130 m/s. The measurements were conducted near atmospheric pressure, however liquid and air preheats to 400 K and 450 K could be provided. Air to the laboratory rig flowed from a Reliance multi-stage axial blower and heating was provided by a Chromalox in-line electrical resistance air-heater. This system was designed to deliver an air mass flow rate of 1.17 kg/s at maximum blower output.

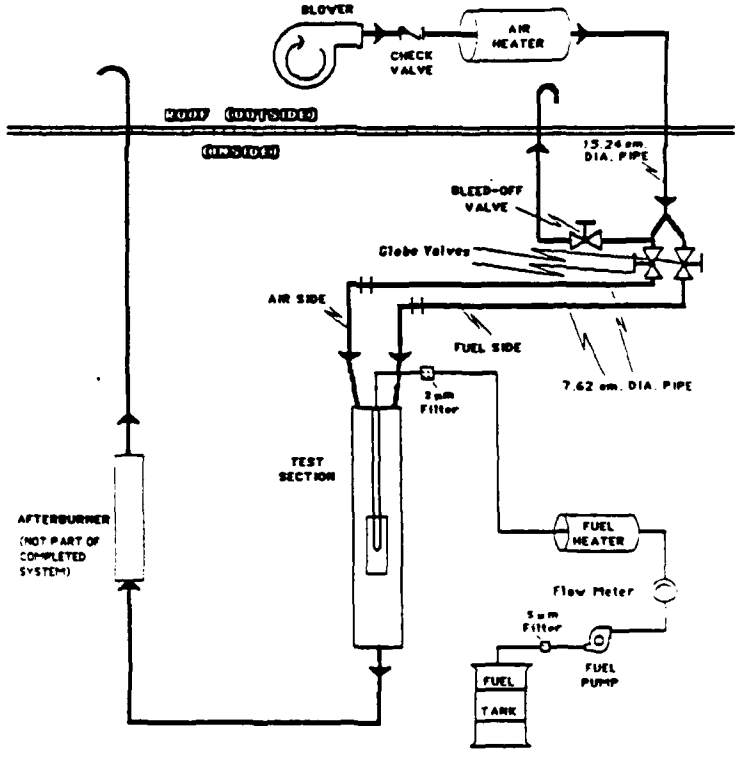

Figure 1. Overall system schematic

As noted earlier, a flat prefilming airblast atomizer (with a porous plug at the end) was located inside the test section of the wind tunnel. Upstream of and adjacent to the injector, a splitter plate physically separated the two settling chambers, one for flow in each side of the splitter plate/injector. This arrangement allowed different air velocities on the two sides of the injector and establishes a shear layer emanating from the nozzle tip as shown in Figure 2. The average flow along the side of the porous plug is labeled as the 'fuel side' (U_{afs}) and the average flow along the other side is labeled as 'air side' (U_{aas}). The difference between the velocities at the two sides at the tip of the injector determines the strength of the shear layer being studied. In addition to boundary layers that develop along the duct walls, sharp velocity gradients are also present downstream of the splitter plate due to a shear layer or a wake.

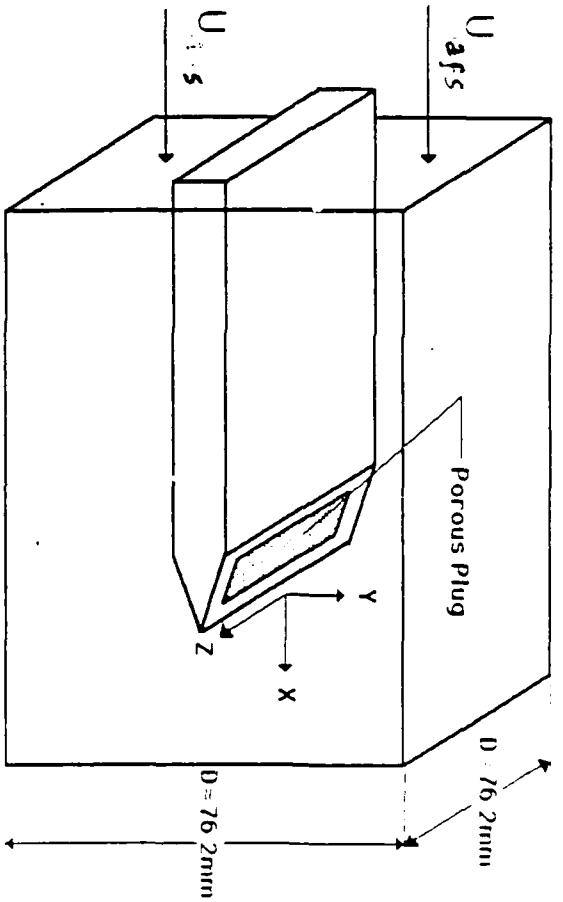

Figure 2. The shear layer formed within the test section

In the present research project, detailed calculations for the evaporating sprays were performed to complement the above experimental program. The experimental and numerical results

provide a basic simplified test bed for the the validation of the characteristic time model. Finite difference calculations for the turbulent flow fields in a confined shear layer were carried out. Calculations for the trajectories and evaporating characteristics for injected droplets were then carried out using a deterministic separated flow model. In addition, the present numerical calculations were extended to give insights to the turbulence-spray interactions viz. the dispersion of liquid droplets due to gas phase turbulence.

Two dimensional steady state predictions of the turbulent shear flows within a vertical duct (similar to the experimental configuration) were obtained. The predictions were used to validate the experimental measurements in addition to extending the range of the parameters considered in the experimental studies. Analysis in the present investigations was limited to dilute sprays; typical of gas turbine combustors. The finite difference calculations of the flow field and spray behavior allows evaluation of the local characteristic times of turbulent mixing and droplet evaporation for comparison with both semi-empirical [Mellor,1980] and the experimental values.

II. ANALYSIS OF TURBULENT SHEAR FLOW IN A DUCT

II.1. General approach

Assuming dilute sprays, calculation of the two dimensional turbulent flow field (neglecting the effects of fuel injection and the fuel insertion device) was carried out first. The ADD code [Anderson et al., 1982] was utilized to perform the calculations . The ADD code along with the PTRAK and VAPDIF codes are among a series of three computer codes developed for predicting the distribution of liquid fuel droplets and fuel vapor in premixing -prevaporizing fuel-air mixing passages of the direct injection type. For a given flow prediction obtained by the ADD code, the PTRAK code predicts the injected fuel droplet trajectories and evaporation characteristics using a deterministic separated flow model. The VAPDIF code (not used in the present research program) predicts the vapor diffusion based on the droplet evaporation characteristics calculated by the PTRAK code. In applying this approach, it is implicitly assumed that the air flow behavior can affect the fuel droplet behavior, but the fuel droplet behavior does not affect the air flow behavior. This is justified when the mass fractions of fuel droplets and fuel vapor are small.

The ADD code was developed to solve the internal flow weak interaction problem using a forward marching numerical procedure that does not require an interaction between the inviscid core flow described by the Euler equations and the boundary layers described by the parabolic boundary layer equations. A forward marching scheme is used to solve the gas phase equations for mass, momentum and energy. An orthogonal coordinate system is constructed for the duct from the potential flow solution such that the stream function forms the coordinate normal to the wall and the velocity potential forms the coordinate tangent to the wall. Since the potential flow streamlines approximate the real streamlines (in a two dimensional sense), the equations of motion may be greatly simplified by assuming that the velocity normal to the potential flow streamlines is small compared to the streamwise velocity. This procedure reduces the governing viscous flow equations to a parabolic system of partial differential equations which can be solved by a forward marching numerical integration procedure. This procedure is attractive when a long tunnel needs to be simulated. For the present calculations, all calculations were done for a rectangular (two dimensional) flow domain with straight duct walls. Hence the orthogonal streamline coordinates generated by the ADD code were identical to the Cartesian (x - y) coordinates.

The basic parabolized compressible Navier Stokes equations solved by the ADD code are given by Anderson and Edwards [1981] and are not repeated in this report.

II.2. Turbulence model

For prediction of the turbulent shear flow, time-averaged conservation equations were considered in the analysis. Various turbulence models have been proposed for the closure of the time -averaged equations in the past. One disadvantage of time averaging is that some important details of turbulent flows (e.g coherent structures) are lost in the predictions. However, depending on the sophistication of the turbulence model used, mixing characteristics and measurable time averaged quantities (e.g. the turbulence intensity and the length scales) can be predicted with the time-averaged conservation equations with reasonable computing times. Some of these quantities have been used in the calculation of characteristic mixing times in turbulent shear layers [Mellor, 1980].

The algebraic turbulence models based on Prandtl's mixing length theory are valid for equilibrium turbulent boundary layer and wake flows. In the algebraic models, the eddy viscosity at any point in the flow and hence the turbulent Reynolds stresses are a function only of the local mean flow and not on the flow history. One equation turbulence models such as described by Gibson et al. [1970] and the two equation models of turbulence such as those formulated by Launder and coworkers [1977] were developed to treat nonequilibrium flows in which the turbulent Reynolds stress is a function of the flow history. A two equation model (k - ε) incorporated into the ADD code was used for the present predictions. The model was originally developed by Jones and Launder [1972], modified for streamline curvature effects by Launder et al. [1977] and then modified by Chen [1980] for low Reynolds numbers. The turbulent viscosity in the k-ε model is given as

$$\mu_T = C_\mu \rho k^2/\varepsilon \qquad \text{(II.1)}$$

where C_μ is an empirical constant . The model contains other empirical constants in the transport equation for the dissipation rate of turbulence.

The governing equations for the turbulent kinetic energy (k) and its rate of dissipation (ε) in the streamline orthogonal coordinate system (as required for the ADD code formulation) are given in Anderson and Edwards [1981]. For most of the calculations, the empirical constants used in the model are as those given by Chen [1980]. A sensitivity analysis was done for the constant C_μ

for better agreement of the predicted mean and turbulent gas flow quantities with the measured values in the parallel experiments (see Section II.6).

II.3. Initial and boundary conditions for the mean flow quantities

A parabolic formulation of the governing equations along with a k-ε turbulence model was used to obtain the computed flow fields in the duct. A forward marching scheme is used to numerically calculate the flow field. The splitter plate (as shown in Figure 2) was not included in the calculations. The mean and turbulent flow quantities at the end of the splitter plate are prescribed as the inlet boundary conditions.

For the mean flow conditions at the inlet, the x component (streamwise) of the mean velocity distribution needs to be prescribed . The y component (normal) of the mean velocity is not solved in the ADD code formulation (orthogonal streamline cordinate) and hence no inlet distribution is required for it. Any arbitrary distribution of the streamwise velocity distribution can be prescribed. In addition to mean velocities, static pressure and temperature of the incoming flow are also prescribed. For the duct walls, no-slip conditions for the velocity is used. The walls are considered to be insulated. For the calculations presented, the inlet static pressure and temperature of the two streams (on the two sides of the splitter plate) are considered to be the same. Mean axial velocity profiles measured close to the end of the splitter plate are used as the inlet conditions for obtaining flow predictions downstream. For equal average velocities of two streams ($U_{afs} = U_{aas}$) on the two sides of the splitter plate, the inlet velocity profiles are characterized by a wake region (due to the thickness of the splitter plate). For non-equal average velocities ($U_{afs} \neq U_{aas}$) a shear layer is present at the central region in addition to the boundary layers near the duct walls.

Modifications to the ADD code

The ADD code was written for analyzing (straight or curved) duct flows with boundary layers near the duct walls and a core flow region near the center. To resolve the sharp velocity gradients near a wall, a turbulent boundary layer profile is calculated in the ADD code from the prescribed inlet mean velocity distribution [Anderson et al., 1982]. The boundary layer profile utilized in ADD [Coles, 1956] is an empirical formulation. The shape of the turbulent boundary layer is also used in grid distribution along the normal direction. In general, this creates a dense grid

distribution near the duct walls and a coarse distribution near the central region of the duct. For the present flow configuration (a confined turbulent shear layer produced by a splitter plate), dense grids were required at the central region , as well as near the duct wall regions. In order to have sufficient number of grid points near the central region of the duct, a grid stretching parameter (a built-in feature in the ADD code) was utilized. This was suitable for most of the computations performed. However, for very strong shear layers at the central region of the duct, the grid was redistributed at the core region to increase the number of nodes at the central region of the duct. This was done without disturbing the grid distribution near the wall .

A typical mesh (uncorrected) produced by the ADD code (for a prescribed inlet flow distribution with a shear layer at the central zone) is shown in Figure 3 where 13 x 55 (x x y) grid is used. Figure 4 gives the redistributed computational mesh for the confined shear layer calculations..

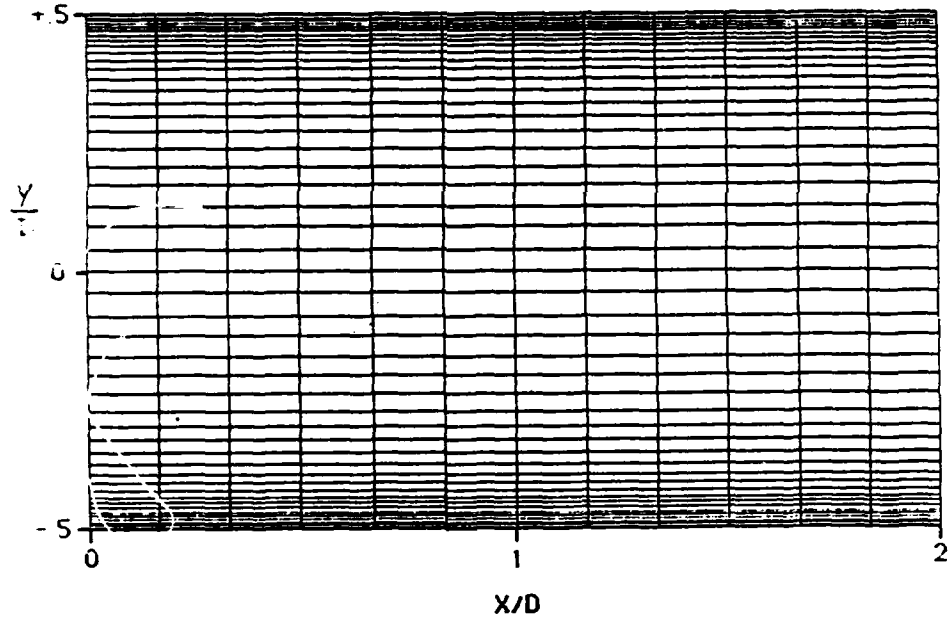

Figure 3. Mesh produced by the ADD code from the inlet flow distribution measured at the end of the splitter plate.

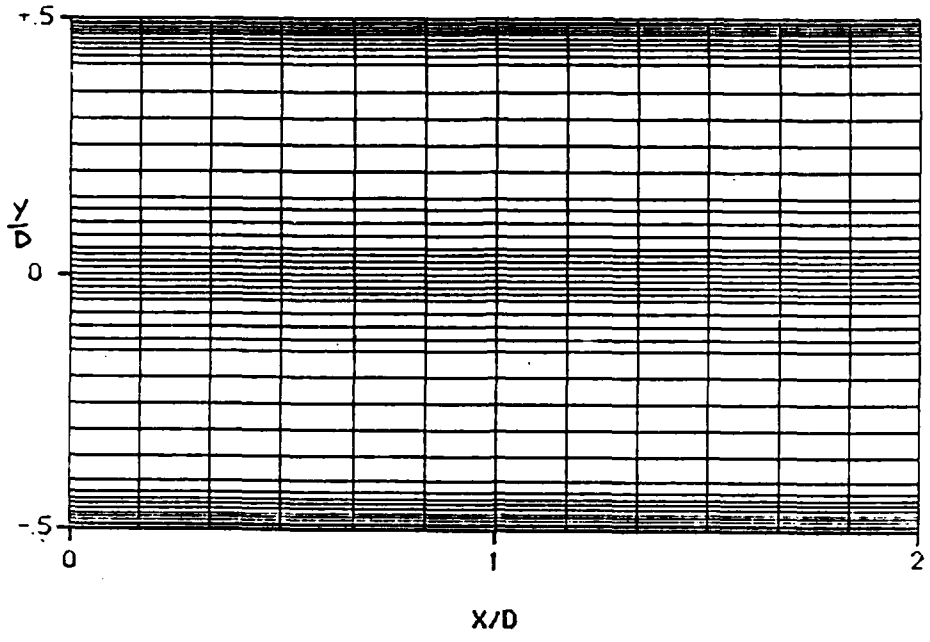

Figure 4. Modified mesh for the same initial flow distribution data as in Figure 3.

Most of the results presented in this report were obtained with a redistributed mesh as the inlet flow distribution at the inlet contained a shear layer or a wake at the central region.

II.4. Initial and boundary conditions for the turbulent flow quantities

For the two equation turbulence model used in the study, distributions for k and ε are required at the exit of the splitter plate. These inlet values are not known a priori, even if the mean axial flow distribution is specified. For the present calculations, the inlet values for k and ε were obtained either from the mixing layer theory [Anderson and Edwards, 1981] or derived from experimental measurements of the turbulence intensities and length scales close to the end of the splitter plate. At the duct walls, the values of k and ε were both set equal to zero along the entire length.

Evaluation of k and ε at the inlet from the mixing length model:

The Prandtl mixing length is defined by

$$\mu_T = \rho \ell^2 |e| \qquad \text{(II.2)}$$

where μ_T is the turbulent viscosity and e is the rate of strain. In the region near the wall, the mixing length is modified by the van Driest factor (A^+) which is given by

$$\rho_w u^* \ell / \mu_w = \kappa Y^+ [1 - \exp(-Y^+ / A^+)] \qquad \text{(II.3)}$$

where u^* is the friction velocity

$$\sqrt{\tau_w / \rho_w}$$

Y^+ is the universal distance to the wall ($\rho_w u^* y / \mu_w$) and κ is the von Karman constant.

In the outer region of the turbulent boundary layer, including the free stream,

$$\mu_T = \rho \ell u_{max} \qquad \text{(II.4)}$$

where the mixing length is given by

$$\ell = \chi \delta^* \qquad \text{(II.5)}$$

δ^* is the displacement thickness of the turbulent boundary layer and the proportionality constant χ is determined by Clauser [1956] to be equal to 0.016. The initial conditions for k and ε are then given as (within the boundary layer):

$$k = \gamma \mu_T |\Sigma| / (C_\mu^{0.5} . \mu_E . \rho) \qquad \text{(II.6)}$$

and

$$\varepsilon = \gamma \mu_T |\Sigma^2| / (\mu_E^2 . \rho) \qquad \text{(II.7)}$$

where $\mu_E = \mu + \mu_T$ and γ is an intermittency factor given by Klebanoff [1954] to reduce the turbulence to zero at the edge of the boundary layer:

$$\gamma = \left[1 + 5.5 \left(\frac{y}{\delta}\right)^6 \right]^{-1} \qquad \text{(II.8)}$$

The boundary layer thickness δ is taken as halfwidth of the duct.

Σ is the streamwise stress distribution at the inlet (obtained from the prescribed or measured inlet flow profile. For the present flow calculations Σ reduces to (due to straight duct)

$$\Sigma = \mu_E \frac{\partial U}{\partial y} \qquad \text{(II.9)}$$

where U(y) is the mean axial flow distribution at the inlet.

For a duct flow without a shear layer or a wake (i.e. no splitter plate upstream) , the central region generally has a flat velocity profile (free stream condition). Though such cases were not considered in the present study, the turbulent kinetic energy and dissipation rate can be specified at the inlet for such cases if the turbulence intensity is specified. Thus if I is the turbulence intensity, the turbulent kinetic energy is given as

$$k_\infty = \frac{I^2}{2} U^2_{max} \qquad \text{(II.10)}$$

The free stream dissipation ε_∞ is taken as the value ε in the boundary layer where k in the boundary layer matches k_∞.

Evaluation of k and ε at the inlet from the measurements of the turbulence intensities and length scales at the end of the splitter plate:

Assuming isotropic turbulence, the k and ε values at the inlet of the computational domain can also be evaluated from the measured distributions of the turbulence intensity (rms fluctuations) and the longitudinal length scale L_e. These vlaues were measured (see the final report to ARO Grant Number DAAG29-84-K-0165) close to the splitter plate end at x/D = 0.03 (see Figure 2) as a function of the y direction.

The turbulent kinetic energy is defind as

$$k = 0.5 \left(\overline{u'^2 + v'^2 + w'^2}\right) \qquad \text{(II.11)}$$

where u' , v' and w' are the fluctuating velocity componenets at the x, y and z directions. For isotropic turbulence,

$$k = 2/3\,\overline{u'^2} \qquad \text{(II.12)}$$

From Jones and Launder [1972], the length sacle L_e may be derived from the definitions of k and ε as:

$$L_e = C_\mu^{3/4}\, k^{3/2} / \varepsilon \qquad \text{(II.13)}$$

from where the dissipation rate can be expressed as

$$\varepsilon = C_\mu^{3/4}\, k^{3/2} / L_e \qquad \text{(II.14)}$$

Hence from the measured values of turbulent intesities

$$\sqrt{\overline{u'^2}}$$

and L_e along the y direction at the end of the splitter plate, the initial conditions for k and ε can be specified.

II.5. Numerical Methods

The relationship between μ_E and the mean flow are specified through the parobolized governing equations (Anderson and Edwards, 1981) and are solved by a forward marching numerical integration scheme. The equations are first linearized by expanding all dependent variables in a Taylor series expansion in the marching direction (x) and terms of O (Δx^2) are dropped. Finite difference equations are then obtained using the two point centered difference scheme of Keller [1970, 1968]. The resulting matrix equations are block tridiagonal and are solved by block factorization using the method of Varah [1972].

The numerical solution is second order accurate in the y direction, first order in the x

direction and linearly stable. The Δx step size is limited not by linear stability conditions but by required accuracy in the Taylor series expansion in x.

The numerical procedure for solving the governing equations for k and ε is as follows. The procedure involves solving the k and ε transport equations successively in an iterative procedure at each streamwise station and lagging the mean flow equations one step so that the mean flow variables are always known. Furthermore, some of the nonlinear finite difference source terms are arranged on the central diagonal of the tridiagonal matrix to strengthen matrix stability [Anderson and Edwards, 1981].

II.6 Results and discussion

The computations carried out for the turbulent shear flows within the duct closely parallel the series of experimental measurements performed under ARO Grant No. DAAG29-84-K-0165. Table 1 lists the cases for which measurements were done for the mean gas velocities, the turbulence intensity (rms velocity),

$$\sqrt{\overline{u'^2}}$$

and the length scale L_e at various axial locations.

Table 1

Gas phase (experimental) matrix

CASE	U_{afs} (m/sec)	U_{aas} (m/sec)	λ
1	91.4	91.4	0.0
2	91.4	18.1	0.67
3	91.4	0.0	1.0
4	54.8	27.6	0.33
5	91.4	46.0	0.33
6	122.0	61.5	0.33
7	54.8	54.8	0.0
8	122.0	122.0	0.0
10	105.0	105.0	0.0
11	105.0	85.9	0.1
12	105.0	70.0	0.2
13	122.0	122.0	0.0
14	91.4	60.9	0.2

Detailed measurements of mean and turbulent quantities for the above cases can be found in the final report of ARO Grant No. DAAG29-84-K-0165. U_{afs} and U_{aas} denote the mean (spatially averaged) gas velocities in the two sections of the duct, separated by the splitter plate (see Figure 2). λ is an indication of the strength of the shear layer defined as

$$\lambda = \frac{U_{afs} - U_{aas}}{U_{afs}}$$

The inlet conditions for the computations were obtained from measurements of U(y) at x/D = 0.03. The initial conditions for k and ε can be evaluated from the inlet mean velocity distribution using the mixing layer theory (as outlined in an earlier section) or they can be obtained from the turbulence intensity and length scale measurements performed at x/D = 0.03. Mean gas

velocities , turbulence intensity and length scale distributions obtained from the turbulent kinetic energy and dissipation rate predictions were compared with the experimental measurements performed at specific downstream locations. The computations were not performed for all cases listed in Table 1 due to the parabolic formulation of the governing equations in the ADD code. In particular, for cases 2 and 3, the shear layer strength is high and it is likely that reverse flow situations may exist at the tip of the splitter plate. Computed results for cases 1, 3, 4, 5, 6, 7 and 8 are presented in this report.

The calculaions are initiated at the exit plane of the splitter plate. A parametric study was carried out to investigate the effects of adjusting the measured length scale values at x/D =0.03 on the prediction of turbulence intensities downstream. The measured length scale values for case 7 was used for this purpose. The parametric study was performed by using the unadjusted measured length scale values, one-half the length scale values and one-quarter of the length scale values (for evaluating the initial values of dissiapation rate of turbulent kinetic energy ε). Comaprisons of the predictions with experimental measurements of turbulence intensities were made at x/D = 1. It was observed that the predicted intensities were directly proportional to the length scale sizes at inlet. The best agreement of the predictions with the experiments were obtained when the inlet length scale values were 1/2 of the measured values near the core flow and 1/4 of the measured values near the shear layer (extending from approximately y/D = 0.15 to y/D = - 0.15). The above adjustment can be justified from the inherent limitations in the computational model resulting from the assumption of isotropic turbulence in the duct flow. All results presented in the section were obtained by using the measured inlet length scale distributions, with the above adjustment.

A relationship between ε and the length scale is provided by equation (II.14):

$$\varepsilon = C_\mu^{3/4} k^{3/2} / L_e$$

The value of C_μ is traditionally held constant and is set equal to 0.09 in k - ε turbulence models. Sonin [1983] reported that the value of C_μ could be calibrated and depends on the nature of the flow regime (wake, free jet, boundary layer etc.). A parametric study was undertaken to obtain a value for C_μ that gave best agreement between the predictions and experiments performed at downstream locations of the splitter plate exit plane. The results indicated that a value of C_μ = 0.571 (corresponding to reducing the value of L_e by a factor of 1/4) gave the best agreement between experimental and computational profiles of turbulence intensity in the shear layer region. However, a value of C_μ = 0.045 provided better agreement in the wall boundary layer. It was also observed that that the turbulence intensity predictions were insensitive to values of C_μ used in the core region of the flow where velocity gradients are smaller.

Figures 5a, 5b and 5c show the comparison of the predicted and measured mean axial velocities along the duct width at the inlet, x/d = 1 and 2 respectively, for case 1. The measured values at x/d = 0.03 are used to generate the inlet velocity profiles for the computations. Similar plots for turbulence intensity

$$\frac{\overline{u'^2}}{U_{max}}$$

at the inlet, x/D =1 and 2 are shown in Figures 6a, 6b and 6c for case 1. U_{max} is the maximum local velocity measured at the inlet (x/d = 0.03). Comparison of the measured and predicted mean velocities and turbulence intensities along the width of the duct are shown in Figs. 7a, 7b,7c and 8a, 8b, 8c for case 4, in Figs. 9a, 9b, 9c and 10a, 10b, 10c for case 5, in Figs. 11a, 11b, 11c and 12a, 12b, 12c for case 6, in Figs. 13a, 13b, 13c, and 14a,14b,14c for case 7 and in Figs.15a,15b,15c and 16a,16b,16c for case 8. The square symbols represent the computed results while the triangles denote experimental measurements

The predicted mean velocity profiles agreed favorably with the measured data in most instances. Previous computations with uncorrected grids (see Section II.3) resulted in poor agreement of measured and predicted values. Computational results of the mean velocity profile at the center consistently fell behind the measured values. This is thought to be due to the simplifications made in the parabolic formulation of the conservation equations. The predicted turbulence intensity

$$\frac{\overline{u'^2}}{U_{max}}$$

profiles were obtained from the turbulent kinetic energy predictions using

$$k = \frac{3}{2}\overline{u'^2}$$

The agreement of the predictions with the measured values is good, considering the inherent limitations of the k - ε model employed in the calculations.

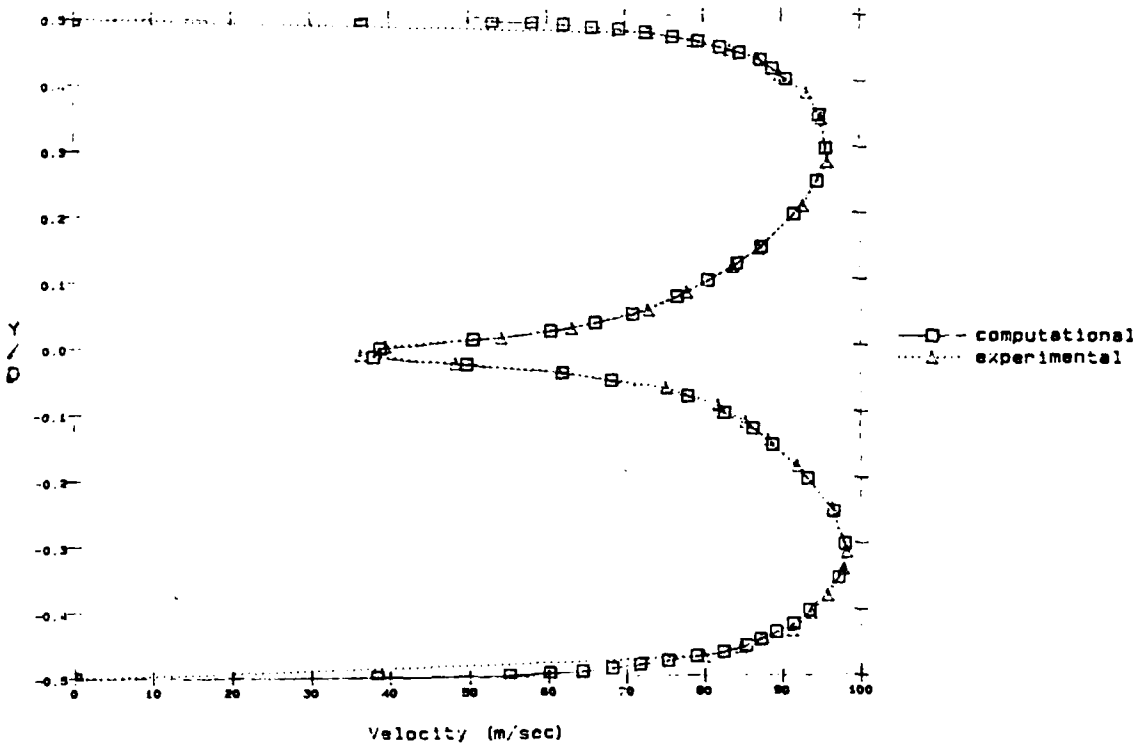

Figure 5a. Comparison of the mean velocity profiles at inlet for Case 1

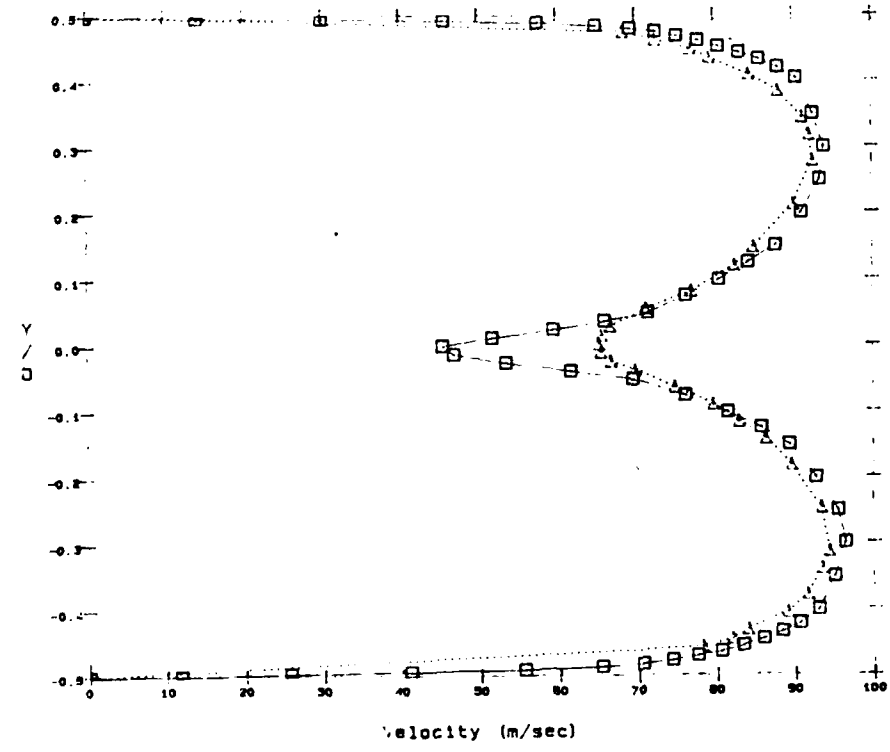

Figure 5b. Comparison of the mean velocity profiles at x/D = 1 for Case 1

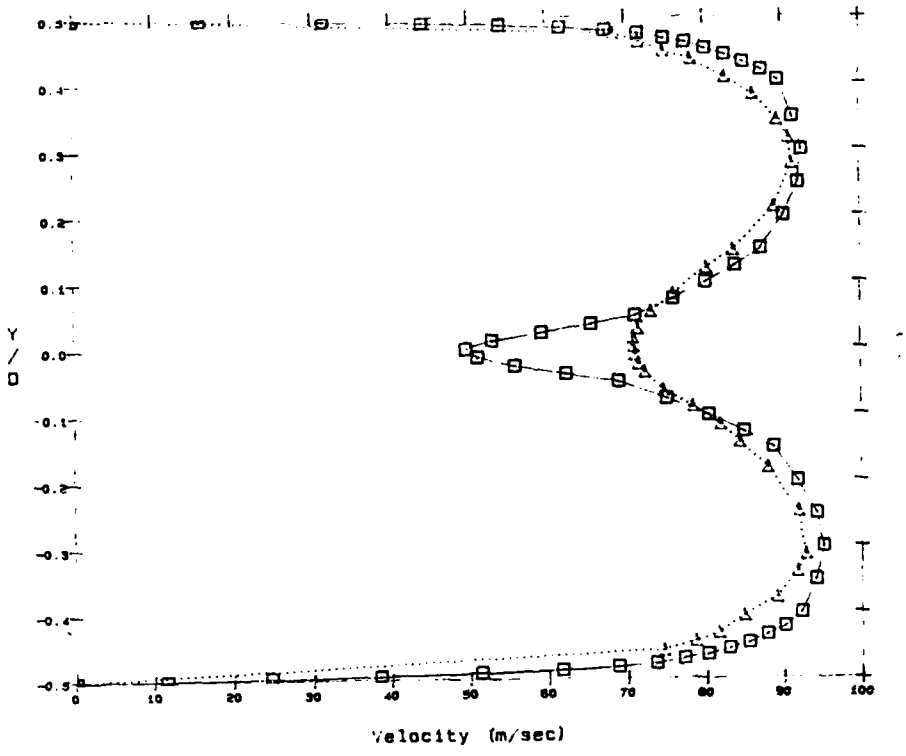

Figure 5c. Comparison of the mean velocity profiles at x/D = 2 for Case 1

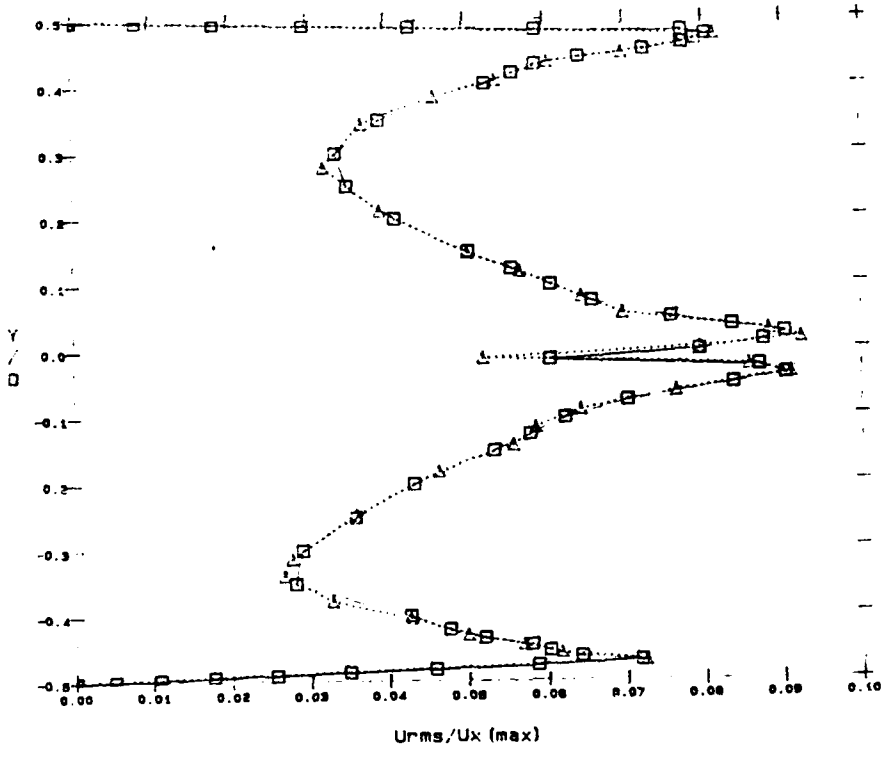

Figure 6a. Comparison of the turbulence intensities at inlet for Case 1

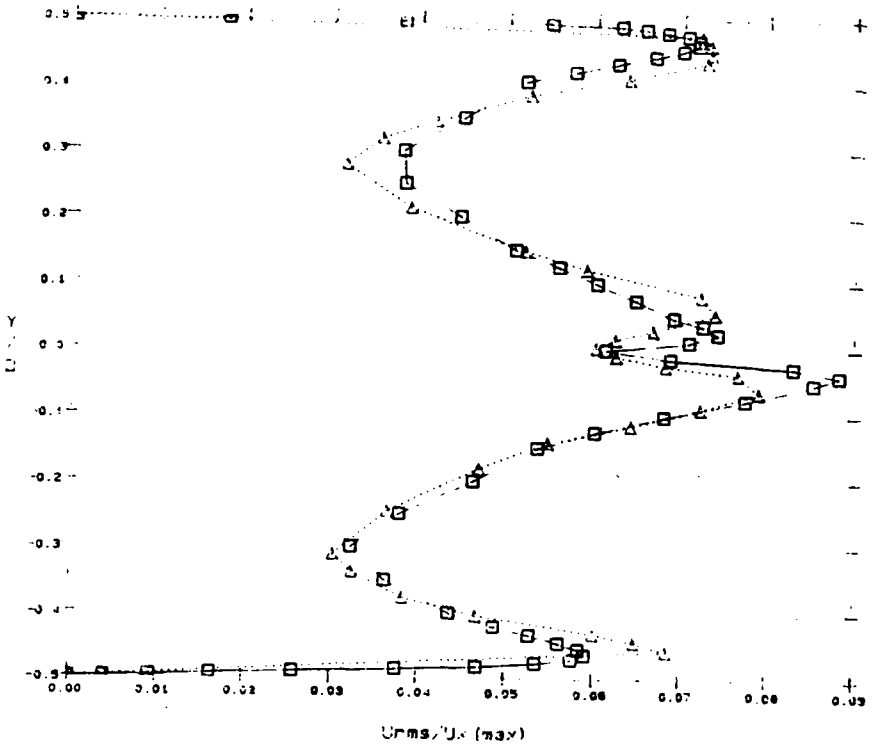

Figure 6b. Comparison of the turbulence intensities at x/D = 1 for Case 1

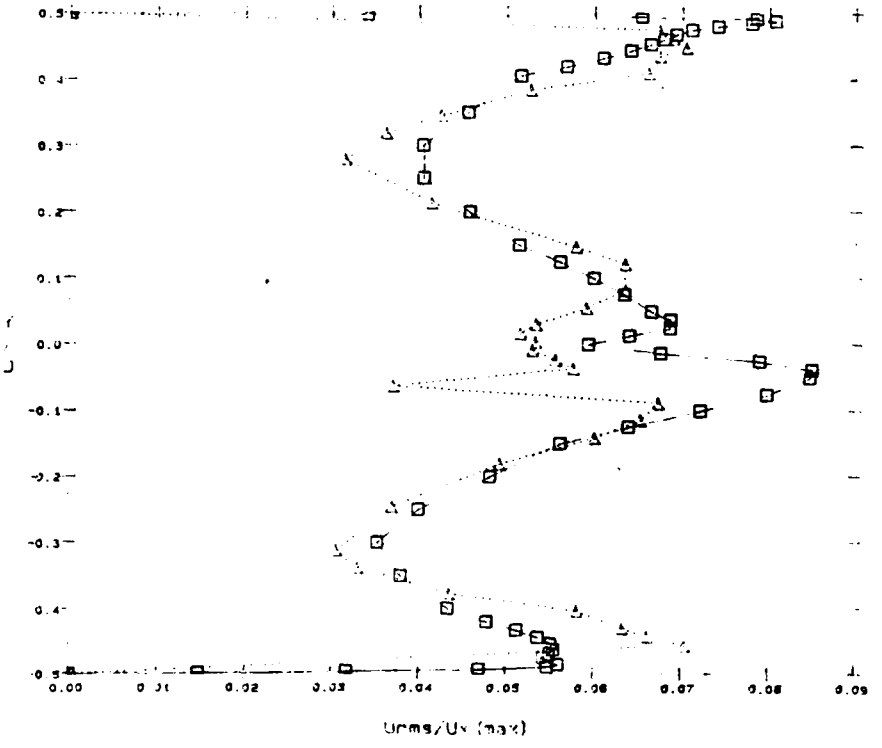

Figure 6c. Comparison of the turbulence intensities at x/D =2 for Case 1

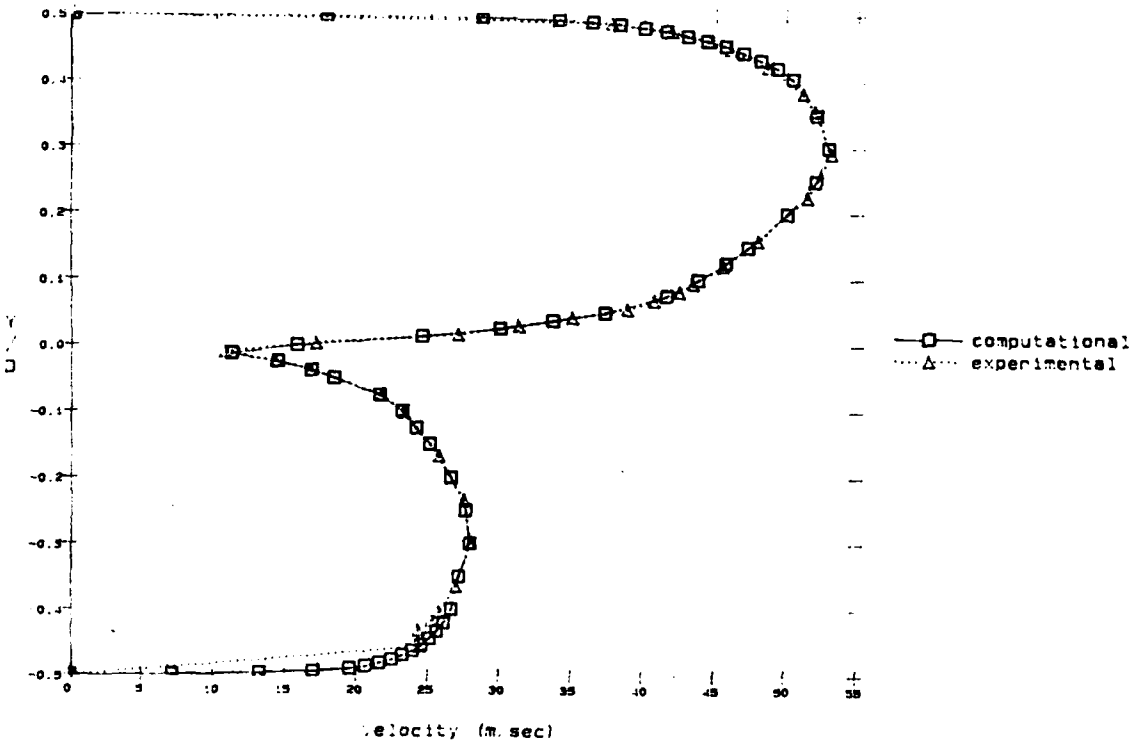

Figure 7a. Comparison of the mean velocity profiles at inlet for Case 4

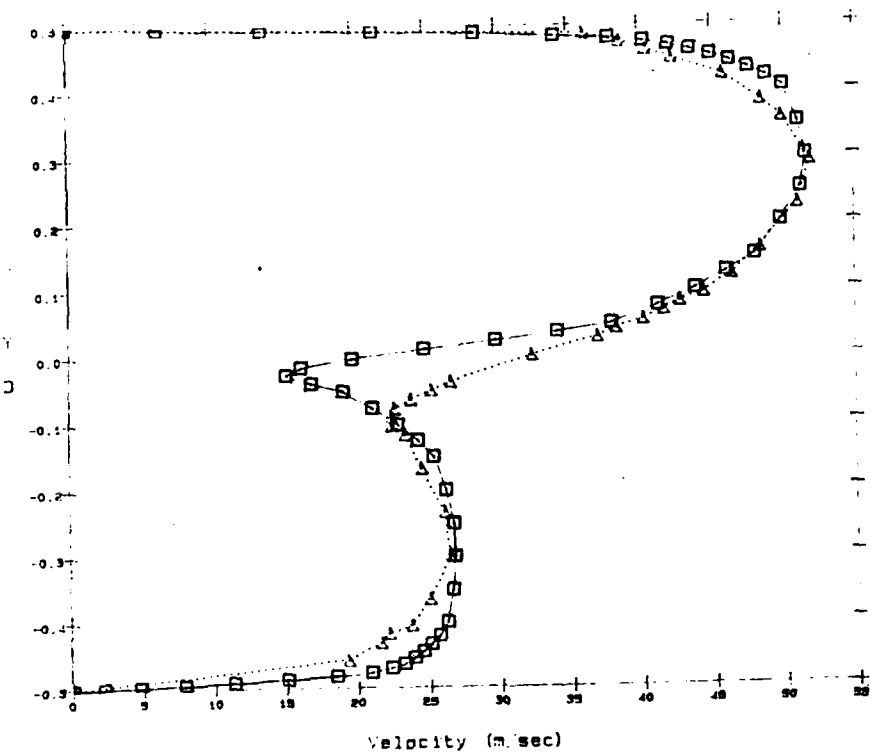

Figure 7b. Comparison of the mean velocity profiles at x/D = 1 for Case 4

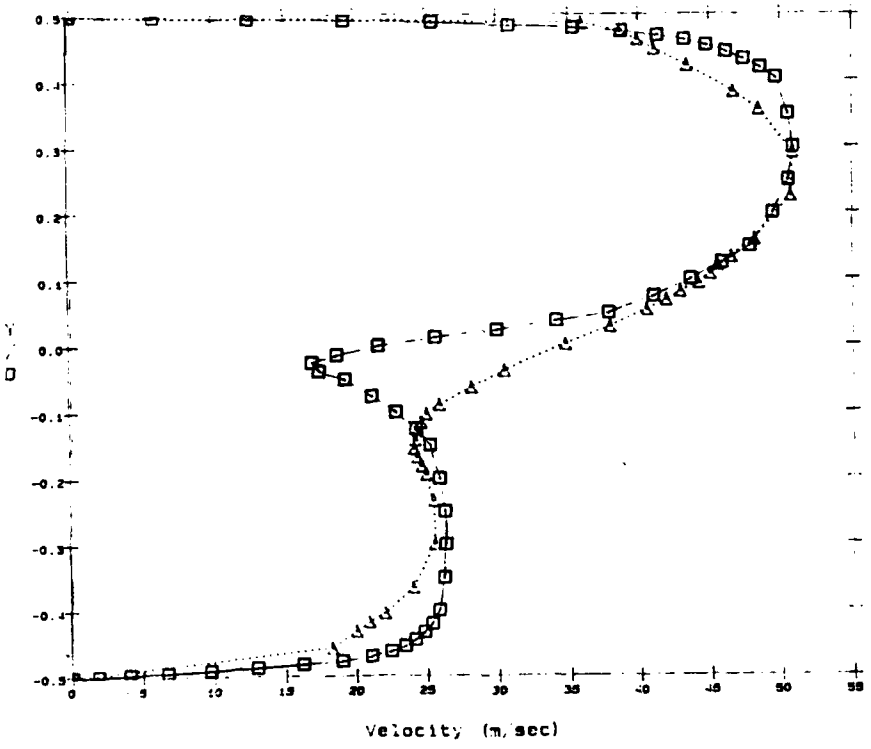

Figure 7c. Comparison of the mean velocity profiles at x/D = 2 for Case 4

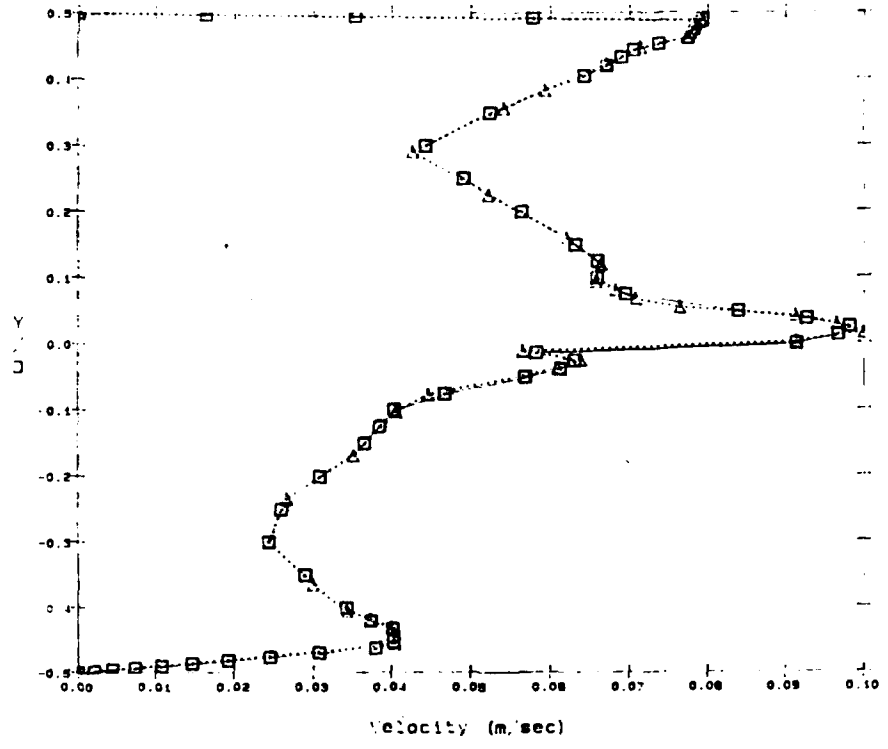

Figure 8a. Comparison of the turbulence intensities at inlet for Case 4

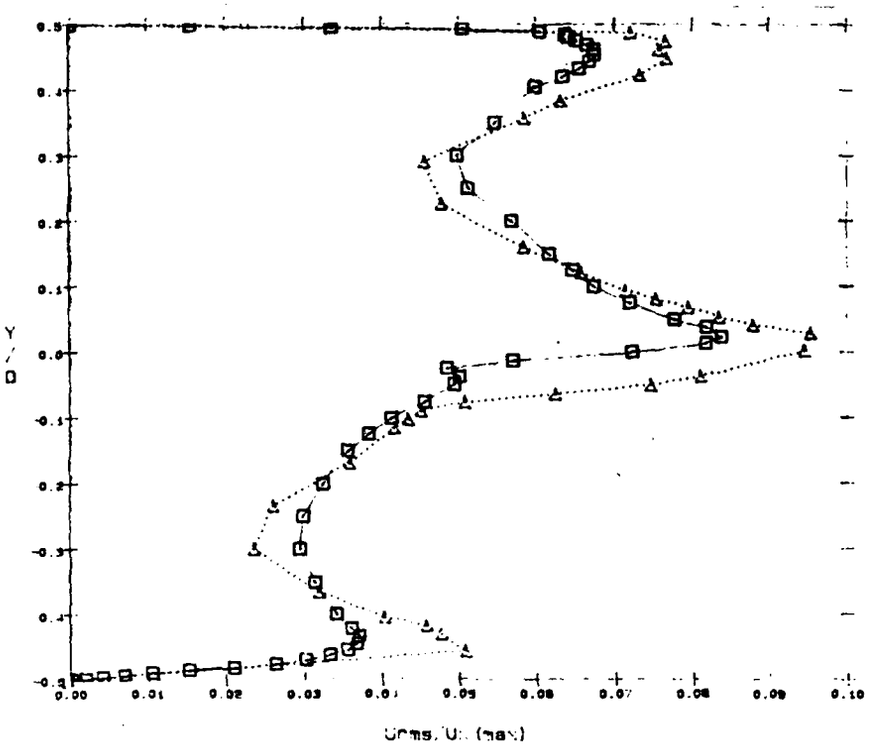

Figure 8b. Comparison of the turbulence intensities at x/D = 1 for Case 4

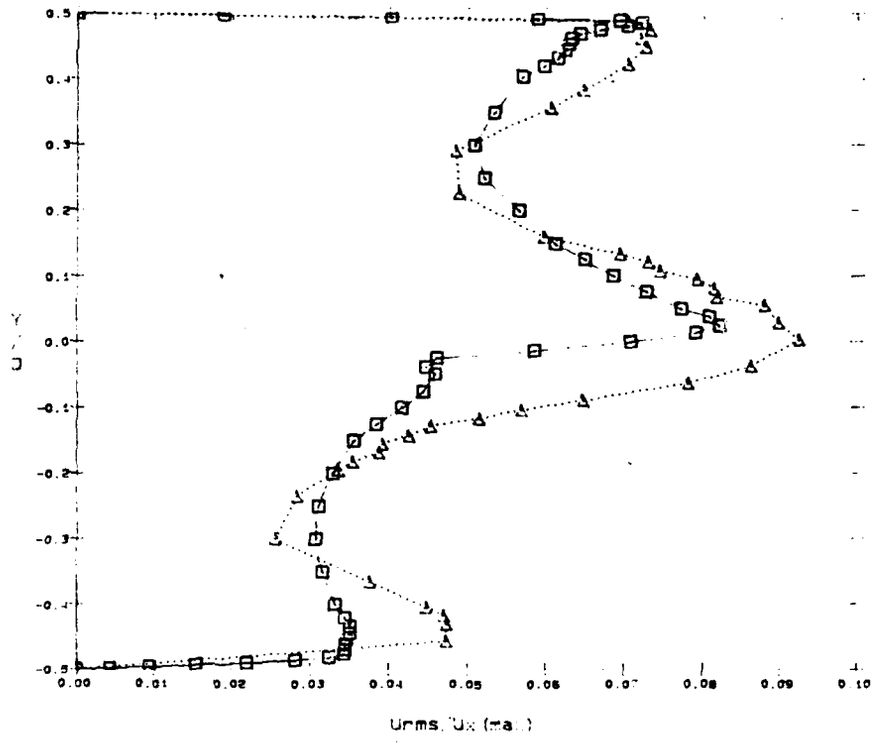

Figure 8c. Comparison of the turbulence intensities at x/D = 2 for Case 4

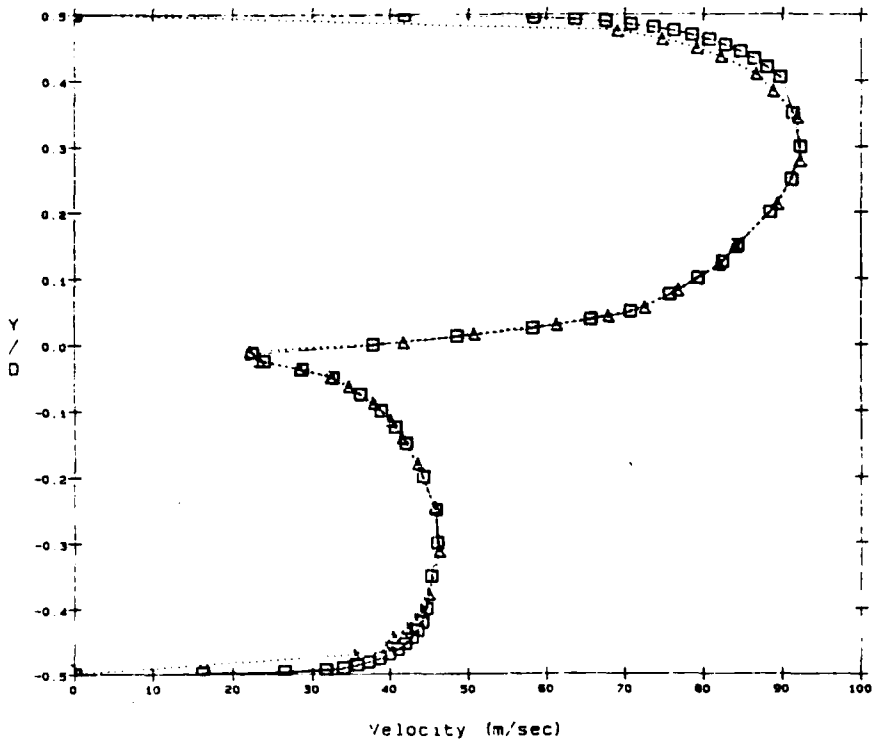

Figure 9a. Comparison of the mean velocity profiles at inlet for Case 5

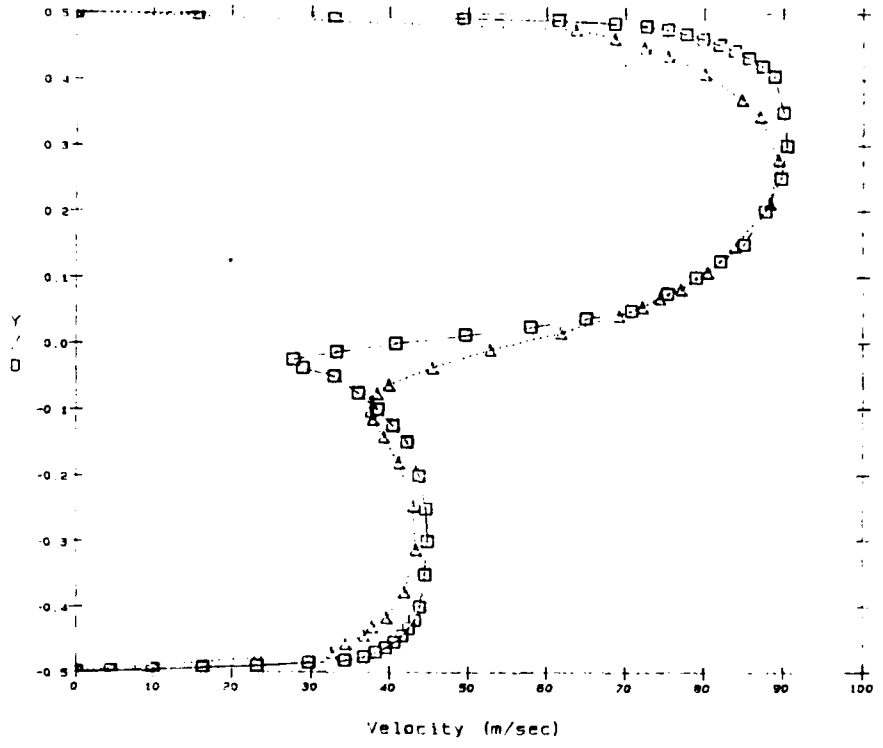

Figure 9b. Comparison of the mean velocity profiles at x/D = 1 for Case 5

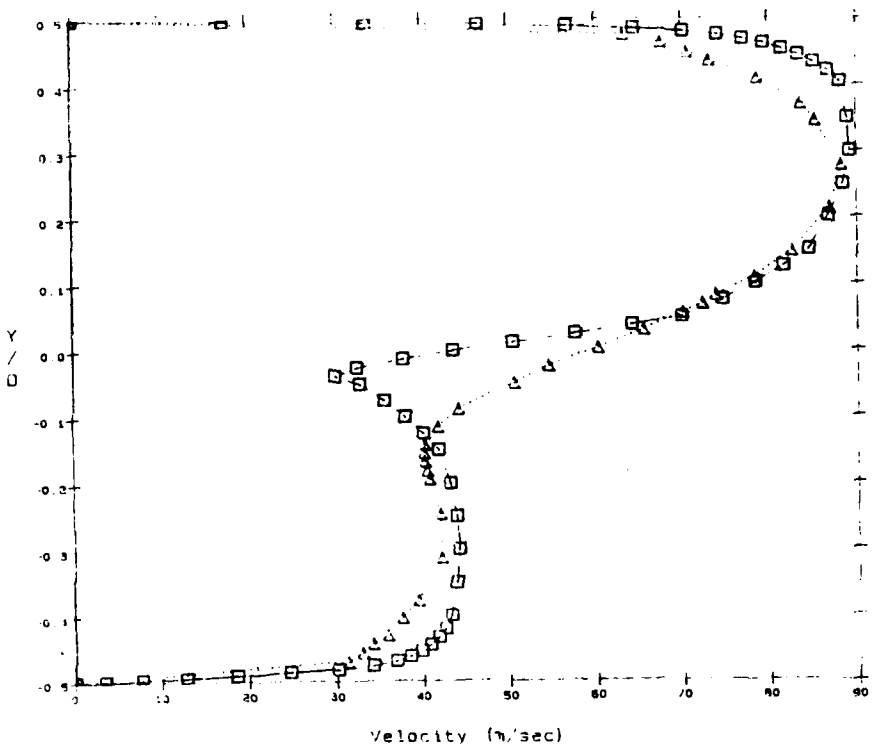

Figure 9c. Comparison of the mean velocity profiles at x/D = 2 for Case 5

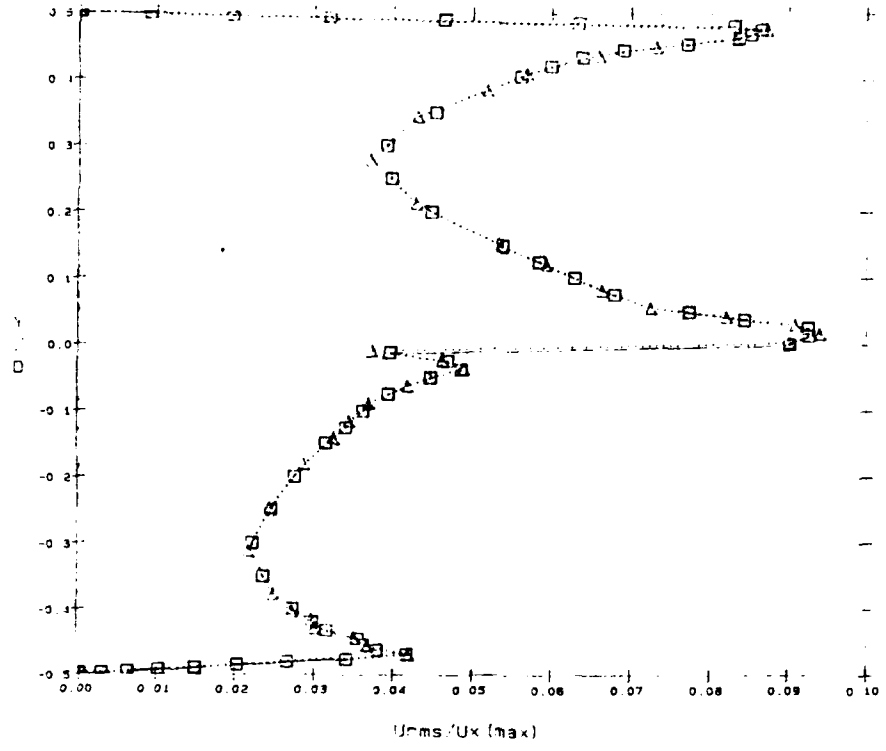

Figure 10a. Comparison of the turbulence intensities at inlet for Case 5

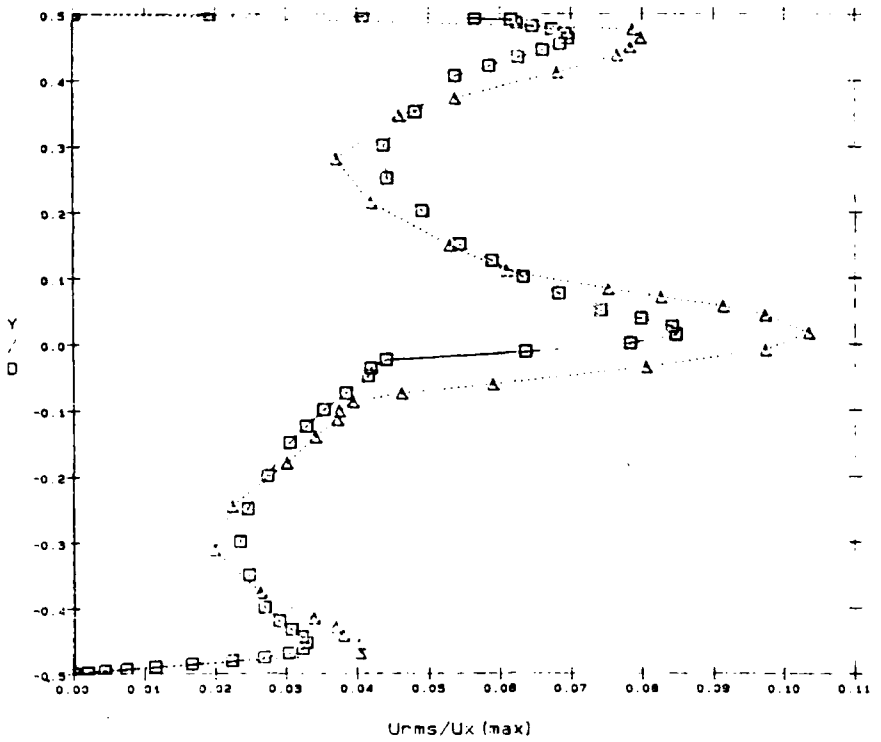

Figure 10b. Comparison of the turbulence intensities at x/D = 1 for Case 5

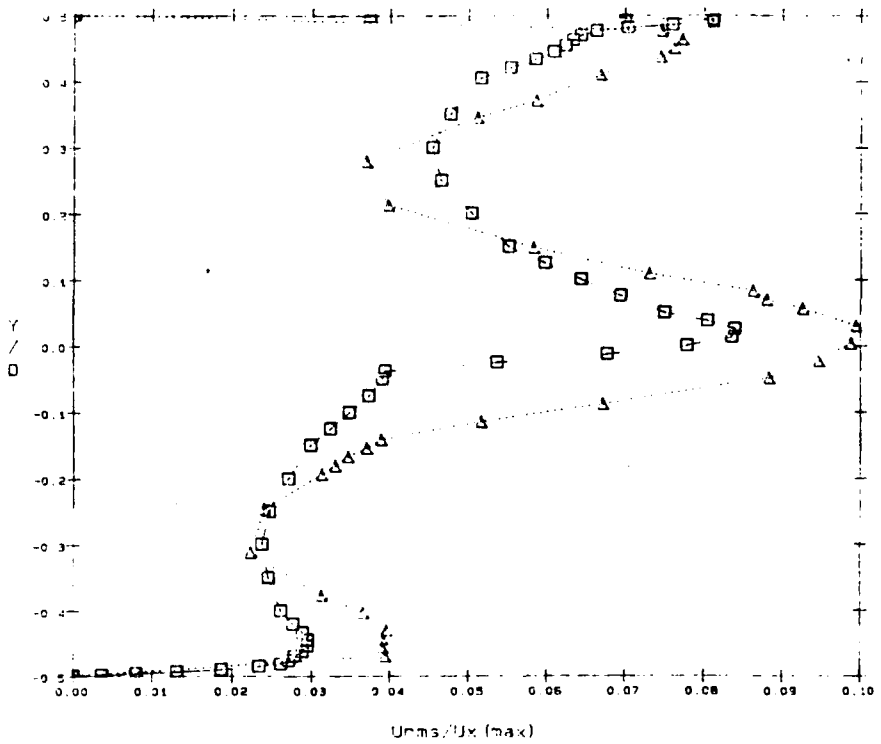

Figure 10c. Comparison of the turbulence intensities at x/D =2 for Case 5

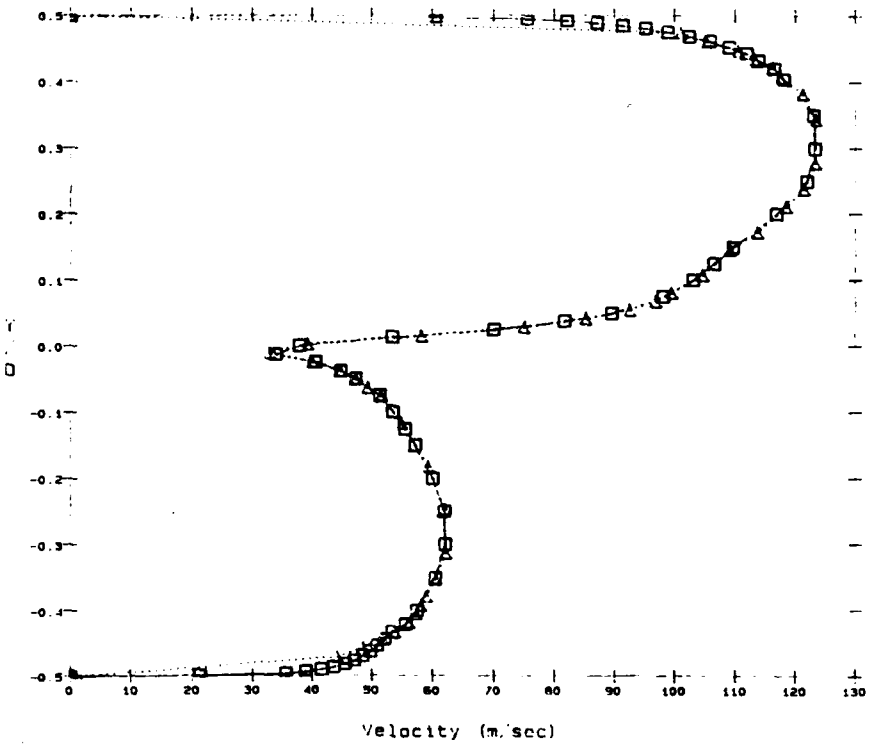

Figure 11a. Comparison of the mean velocity profiles at inlet for Case 6

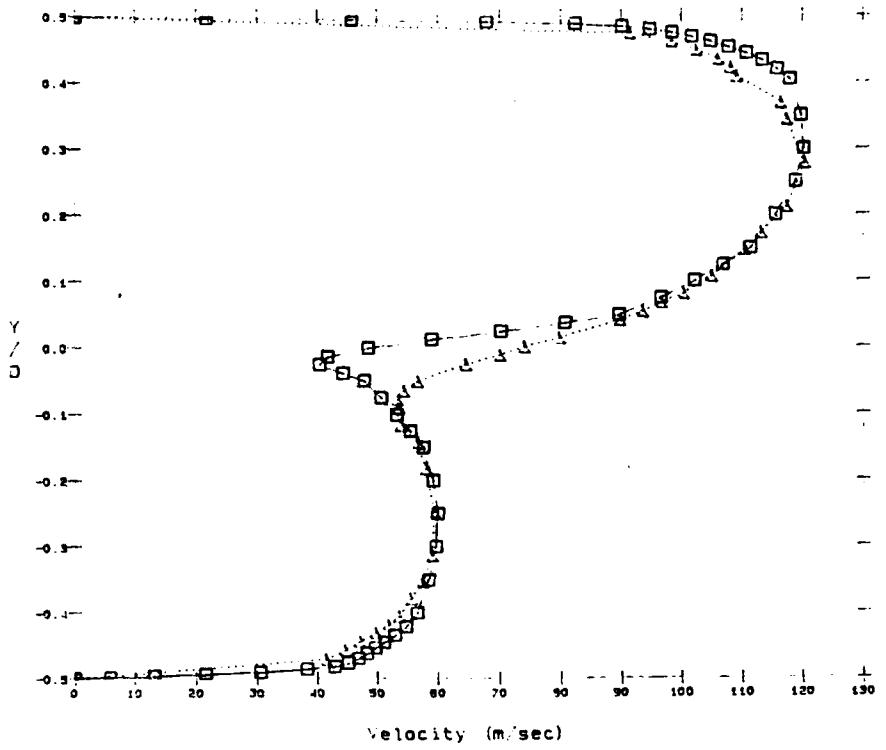

Figure 11b. Comparison of the mean velocity profiles at x/D = 1 for Case 6

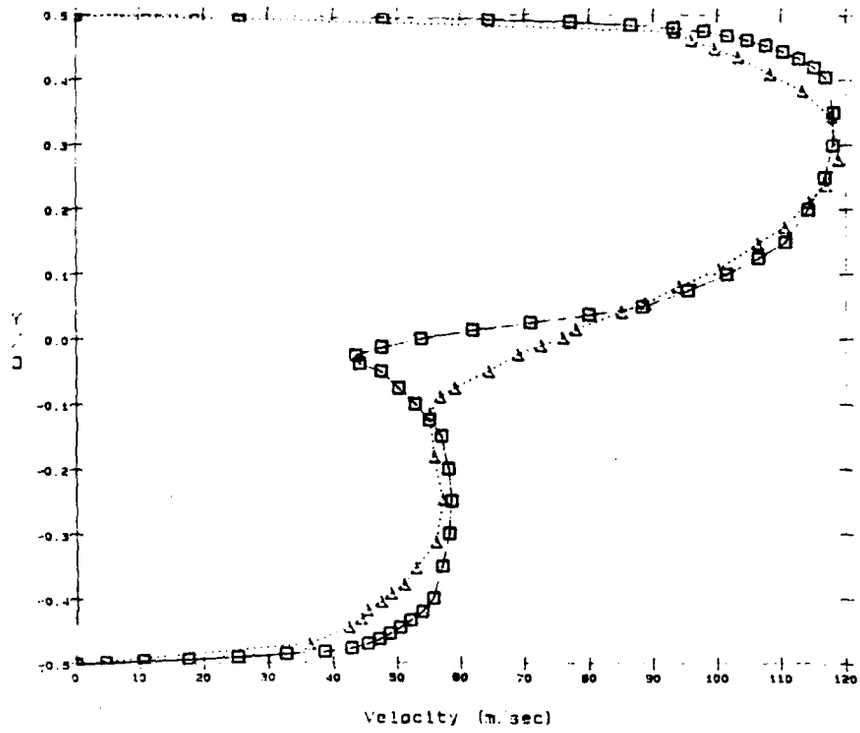

Figure 11c. Comparison of the mean velocity profiles at x/D = 2 for Case 6

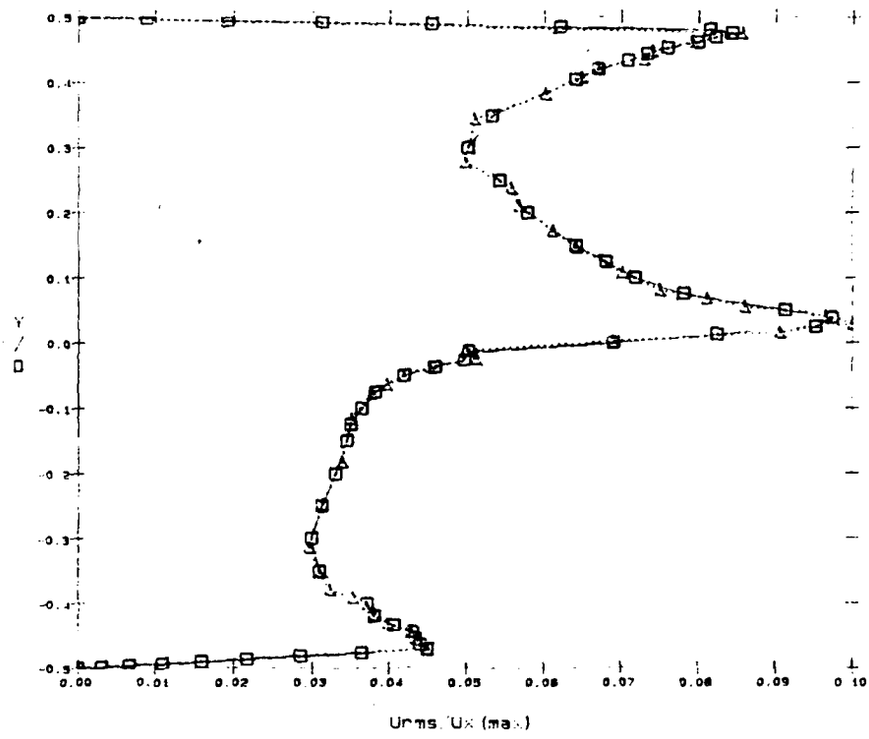

Figure 12a. Comparison of the turbulence intensities at inlet for Case 6

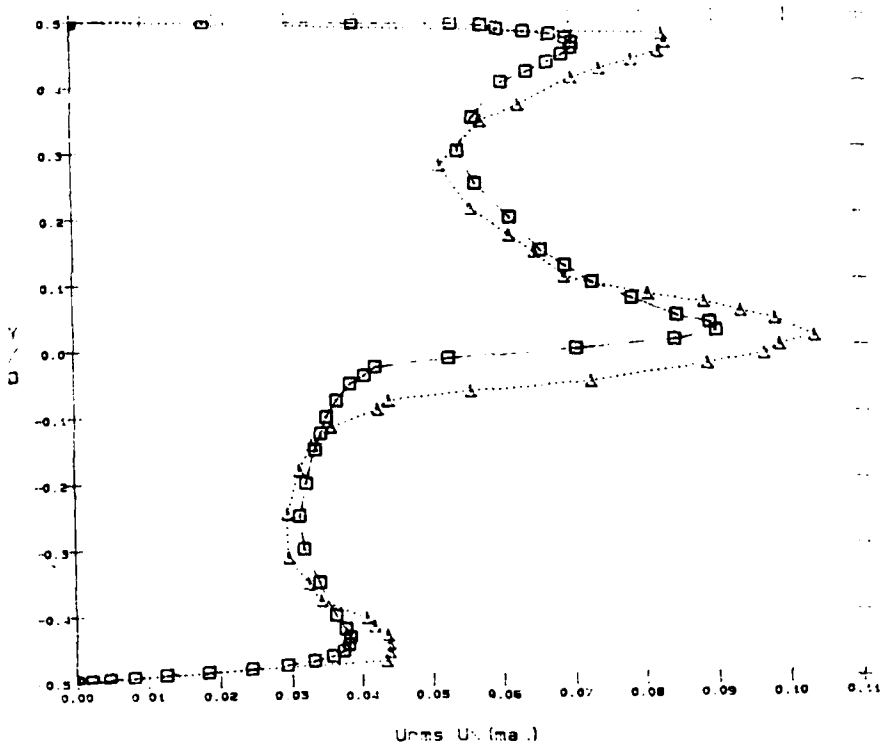

Figure 12b. Comparison of the turbulence intensities at x/D =1 for Case 6

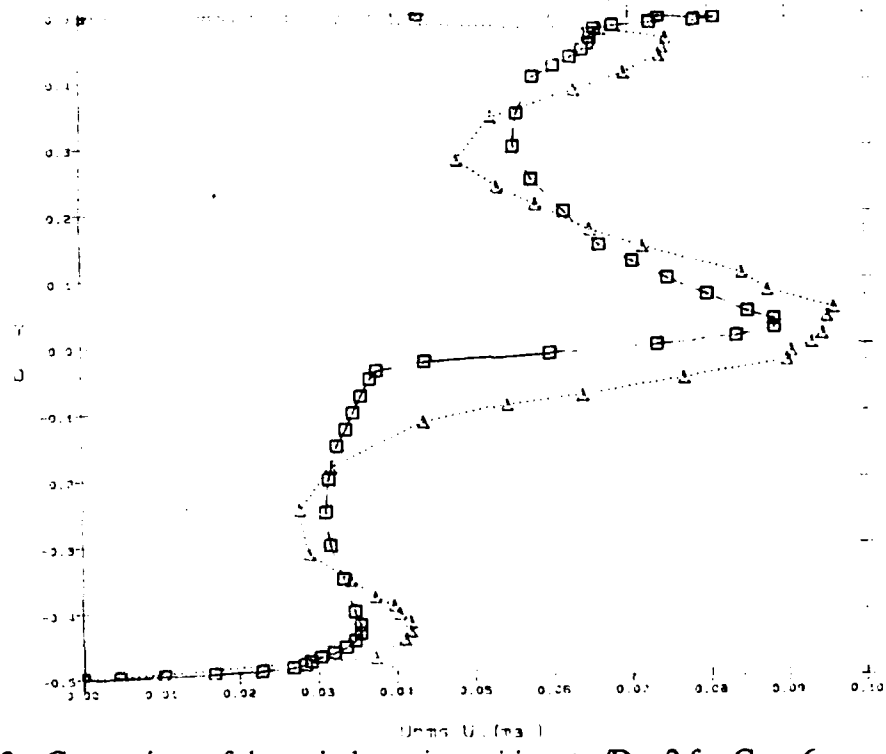

Figure 12c. Comparison of the turbulence intensities at x/D = 2 for Case 6

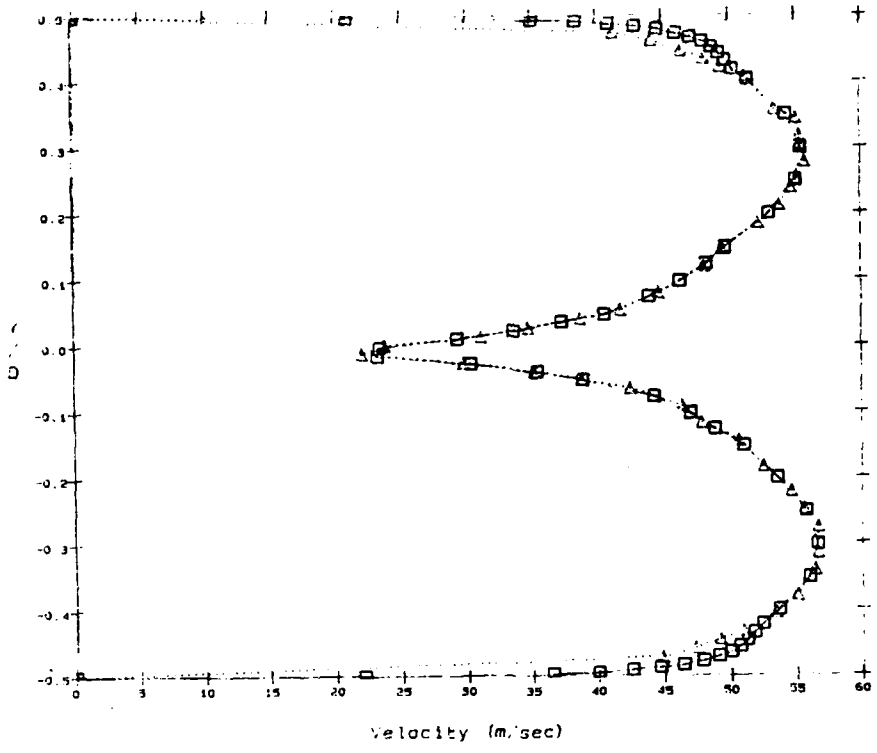

Figure 13a. Comparison of the mean velocity profiles at inlet for Case 7

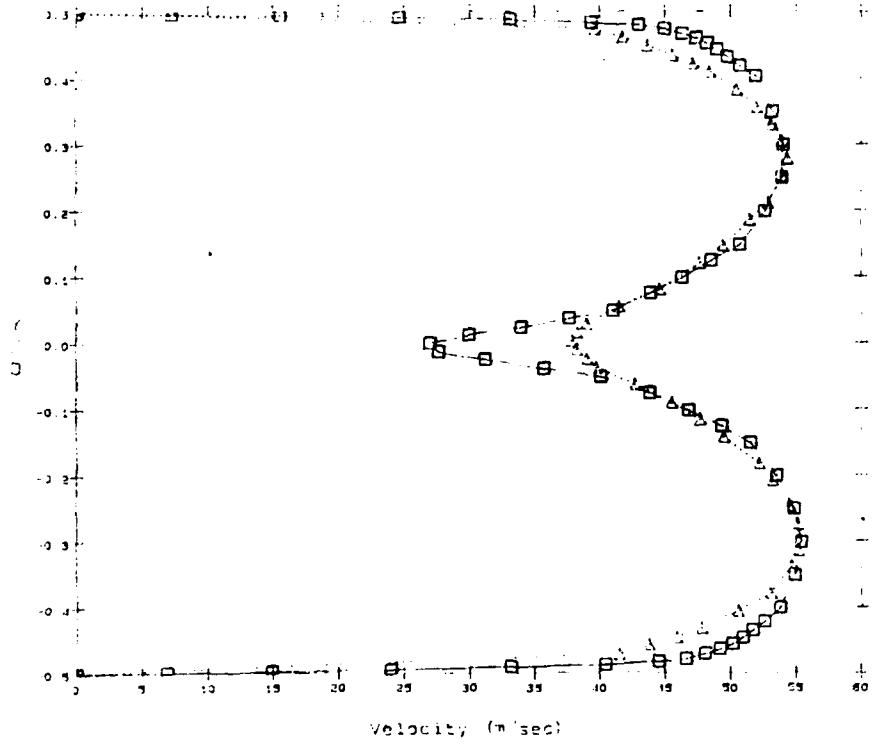

Figure 13b. Comparison of the mean velocity profiles at x/D = 1 for Case 7

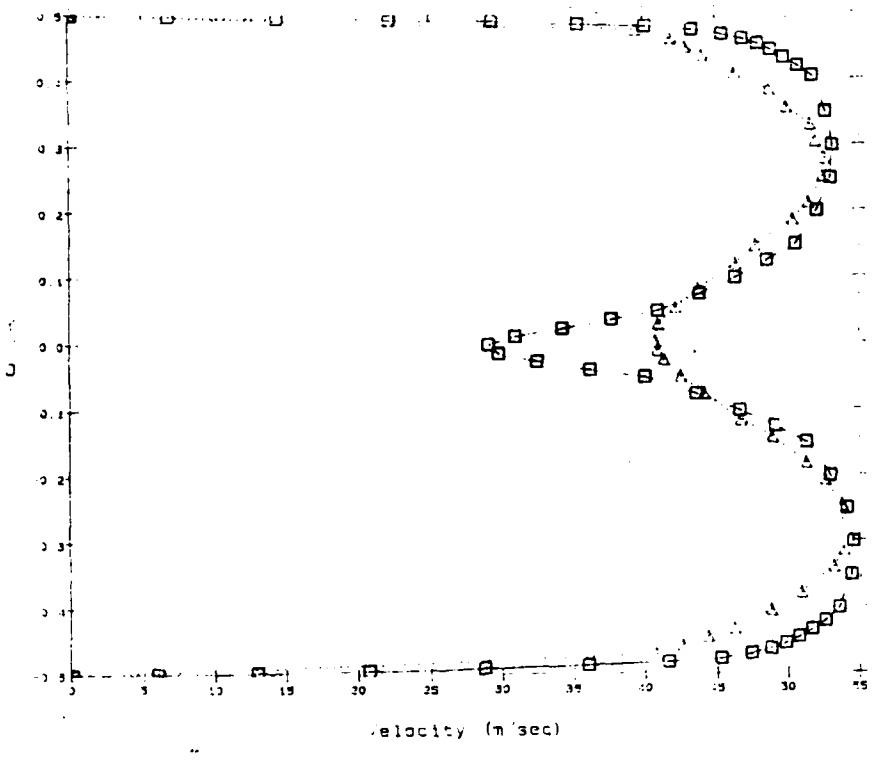

Figure 13c. Comparison of the mean velocity profiles at x/D = 2 for Case 7

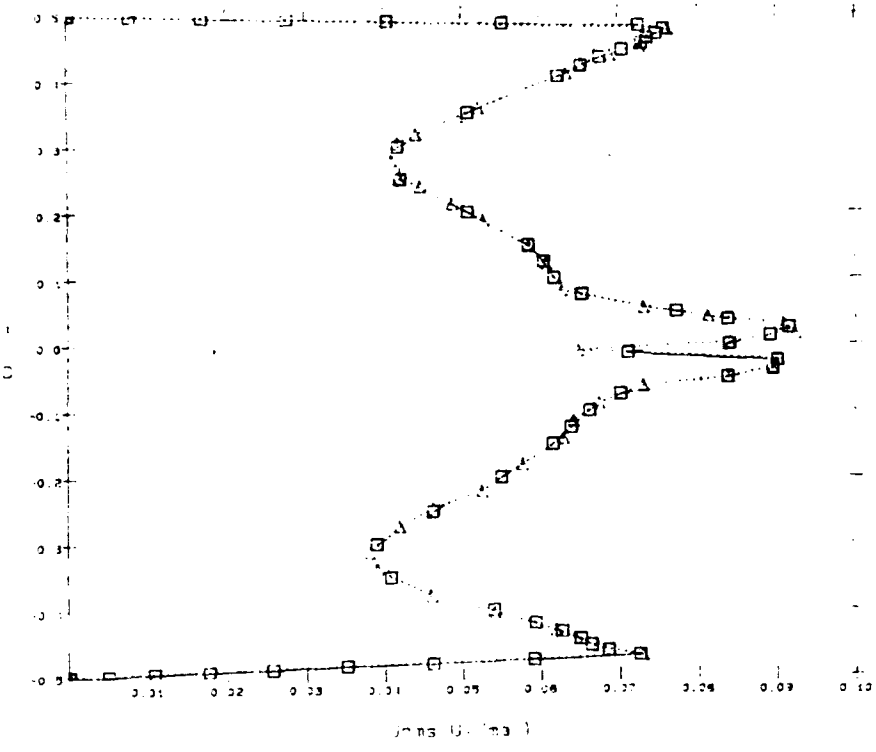

Figure 14a. Comparison of the turbulence intensities at inlet for Case 7

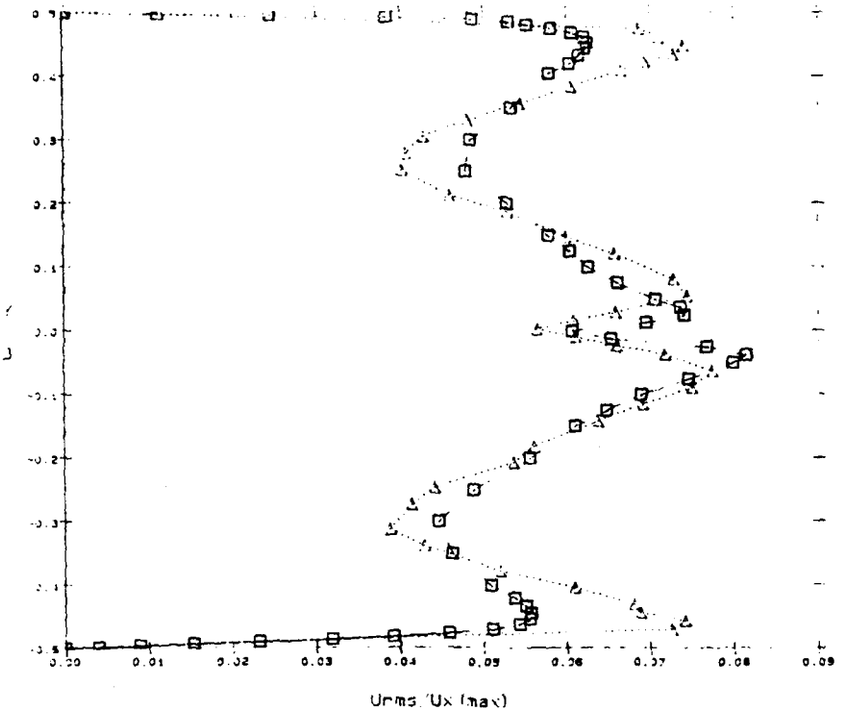

Figure 14b. Comparison of the turbulence intensities at x/D =1 for Case 7

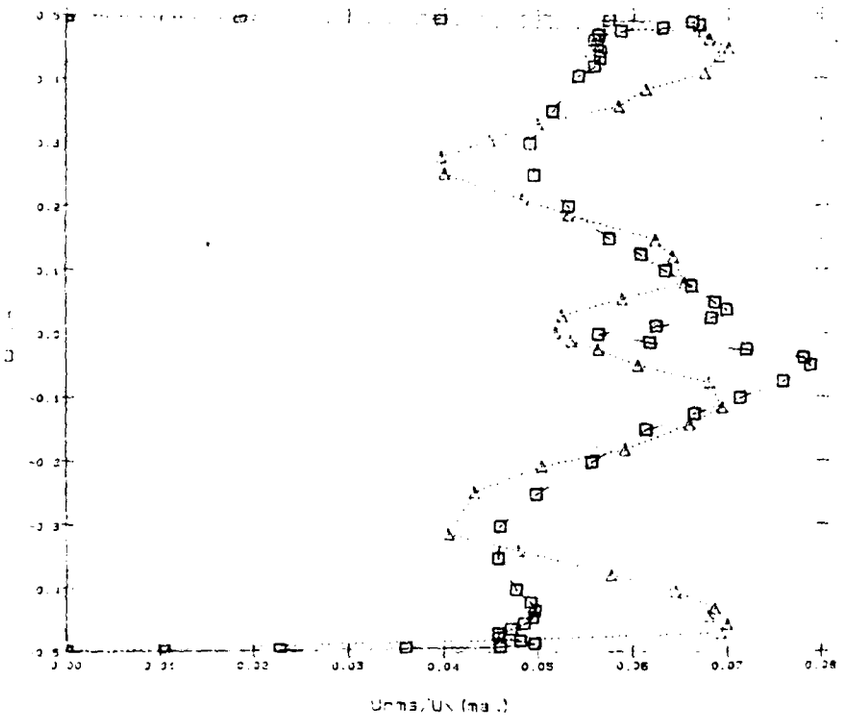

Figure 14c. Comparison of the turbulence intensities at x/d = 2 for Case 7

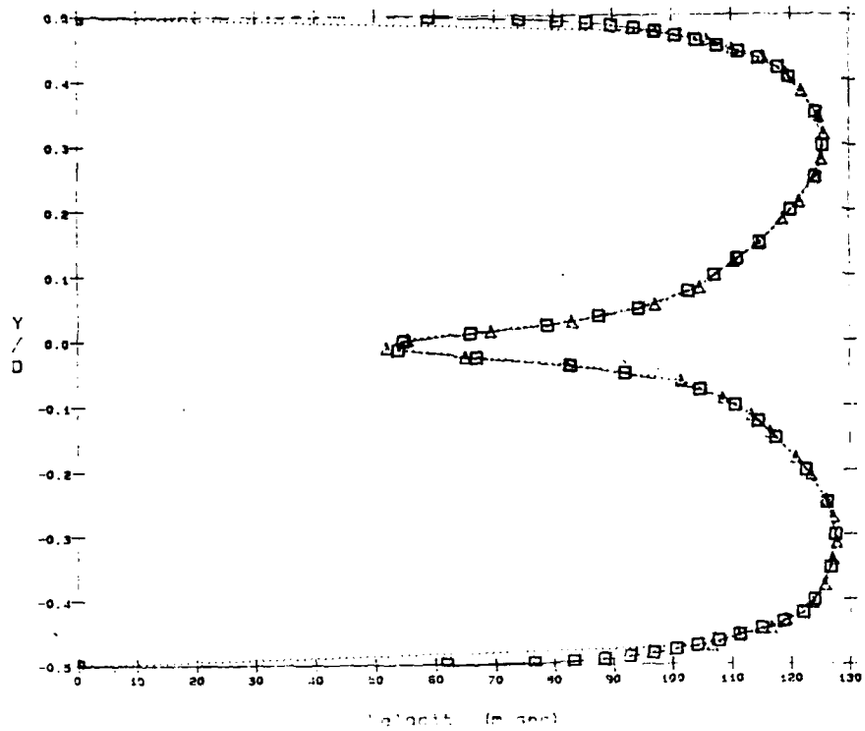

Figure 15a. Comparison of the mean velocity profiles at inlet for Case 8

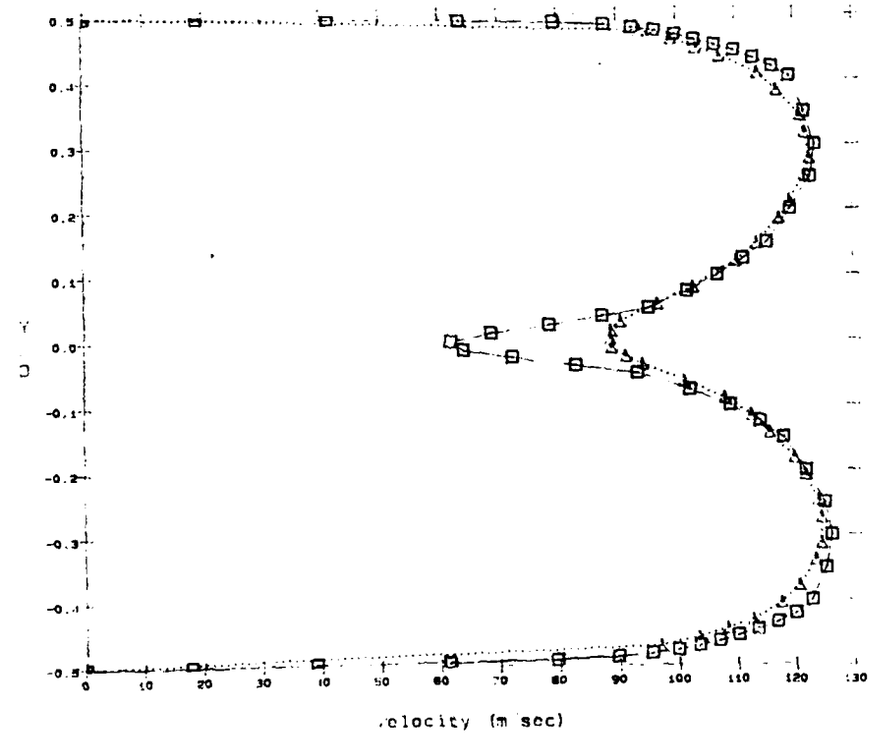

Figure 15b. Comparison of the mean velocity profiles at x/D = 1 for Case 8

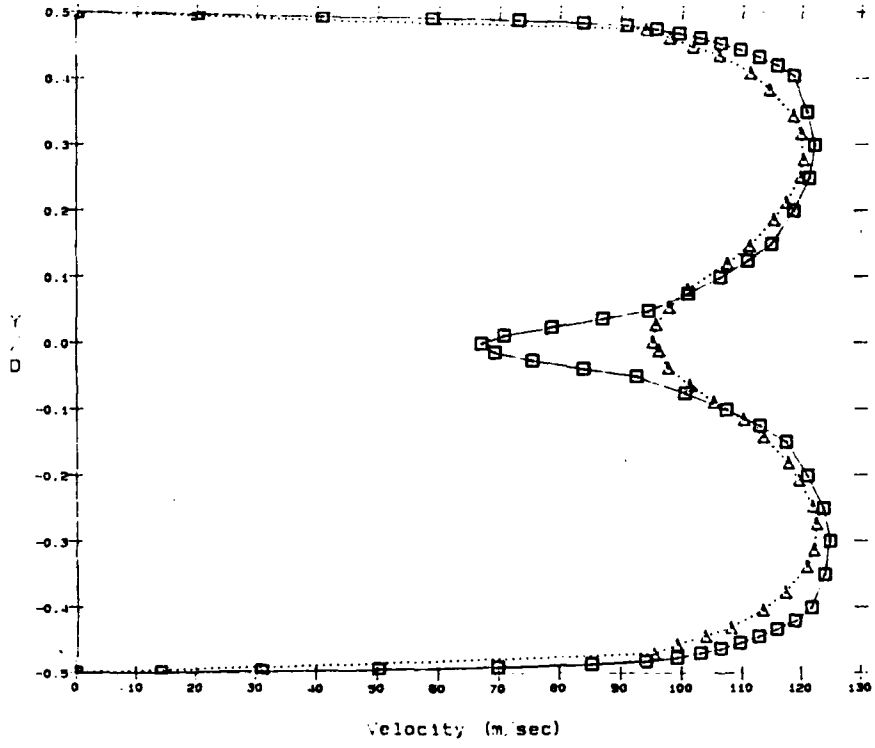

Figure 15c. Comparison of the mean velocity profiles at x/D = 2 for Case 8

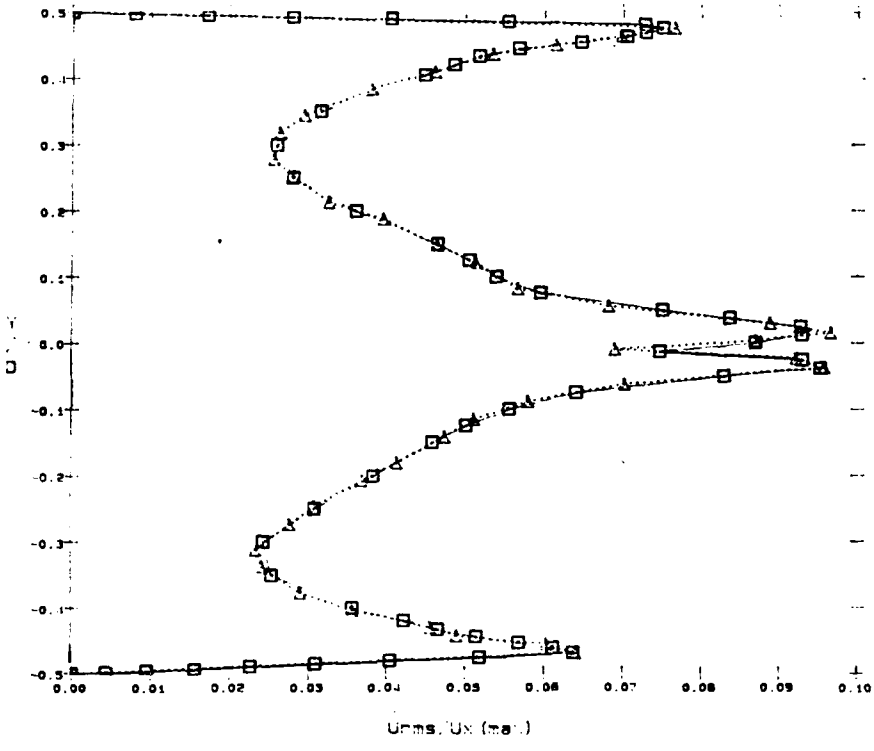

Figure 16a. Comparison of the turbulence intensities at inlet for Case 8

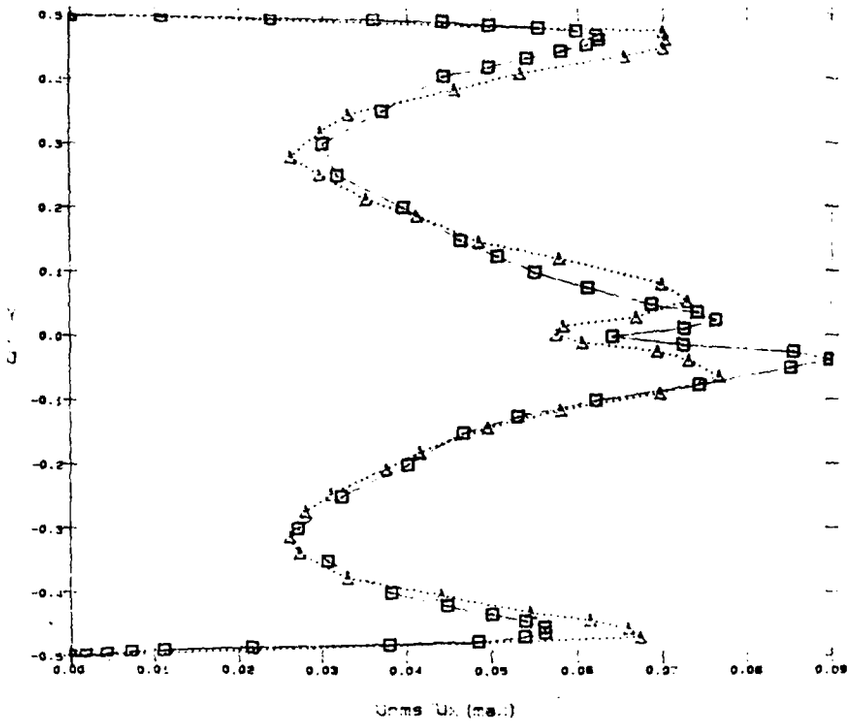

Figure 16b. Comparison of the turbulence intensities at x/D = 1 for Case 8

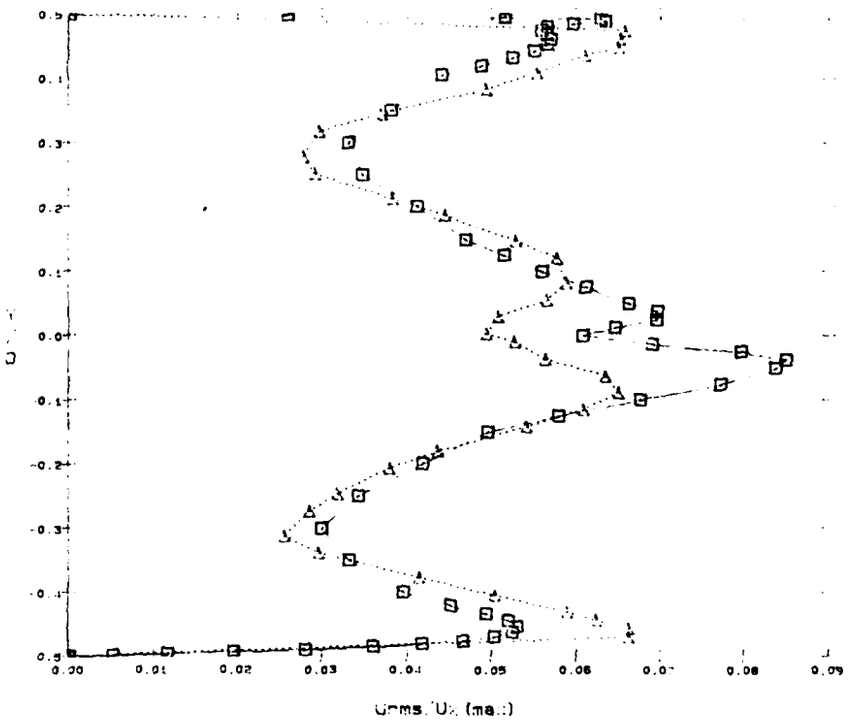

Figure 16c. Comparison of the turbulence intensities at x/D =2 for Case 8

III. ANALYSIS OF DROPLET BEHAVIOR - DETERMINISTIC MODEL

III.1 General approach

The behavior of the fuel spray in the duct downstream of the splitter plate (see Figure 2) is calculated using the PTRAK computer program [Anderson et al.,1982]. The PTRAK code is based on a deterministic separated flow model (mean gas flow variables are only employed for the droplet evaporation characteristics calculation).The code was significantly modified so that the fuel spray behavior can be predicted using a stochastic separated flow model (as described in the next chapter). The droplet dispersion effects due to gas phase turbulence was investigated using the stochastic separated flow model.

The present analyses assumes lean equivalence ratios, i.e., the mass fraction of fuel (dispersed phase) is small. Under these conditions, the air flow behavior is solved first using the method described in earlier sections . The pressure , temperature and mean velocity fields were then stored in data files and used in the fuel droplet analysis. Thus the air flow behavior influences the fuel droplet behavior, but the fuel droplet effects on the gas flow are neglected.

The spray formation processes at the airblast atomizer are not addressed in the present study. It is assumed that the liquid layer on the porous plug (at the end of the splitter plate) disintegrates within a short distance and a spray is formed consisting of droplets that can be characterized by a suitable size distribution. For the present calculations, the spray is assumed to be formed at the inlet of the computational domain. The spray is divided into a number of classes. For each class, droplet diameter, droplet temperature, veocity components and position in the flowfield are specified. These parameters may differ among the various classes. The PTRAK model calculates the trajectory, vaporization rate and temperature variation of each class of droplets. A maximum of 1250 classes can be considered in the PTRAK code.

Droplet shattering and coalescence were not considered in the present study. These features are present in the PTRAK code but are largely untested and without validation. When droplets collide with a duct wall, the predictions can be obtained using any of the two following schemes. Elastic rebounds can be considered or the heat transfer from the wall to the droplets can be considered. Both water (a pure compund) and Jet-A fuel (a distillate liquid) were considered as the dispersed phase.

III.2 Momentum equations

The equations of motion for the fuel droplet trajectories in the Cartesian coordinates are given below.

$$\frac{dU_d}{dt} = \frac{\rho C_d A}{2m_L} \Delta U (U - U_d) \qquad \text{(III.1)}$$

$$\frac{dV_d}{dt} = \frac{\rho C_d A}{2m_L} \Delta U (V - V_d) \qquad \text{(III.2)}$$

where the cross sectional area of the fuel droplet is given by

$$A = \pi d^2/4$$

and m_L is the mass of the droplet. U_d and V_d are the fuel droplet velocitiy components. The drag of the fuel droplet is written in terms of a drag coefficient, C_d.

The relative velocity ΔU is given as

$$\Delta U = [(U - U_d)^2 + (V - V_d)^2]^{1/2} \qquad \text{(III.3)}$$

It is noted that V (the y component of gas phase mean velocity) is identically equal to zero (due to the streamline orthogonal coordinate formulation) according to the ADD code predictions of the gas flow field. In the stochastic separated flow formulation (see next section), the contribution due to the gas phase turbulence is considered in the above equations of motion and U and V are repalced by u and v where (assuming isotropic turbulence)

$$u = U + u'$$

$$\text{and} \quad v = 0 + u'$$

The fluctuating component u' is determined by random sampling of gas phase turbulence properties while droplet motion is calculated using a random walk procedure (see next section)

The drag coefficient is determined from correlations reported by Dickerson and Schuman [1965]:

$$C_d = 27\ Re_d^{-0.84} \qquad 0 < Re_d < 80$$

$$C_d = 0.271\ Re_d^{0.217} \qquad 80 < Re_d < 10^4$$

$$C_d = 2.0 \qquad Re_d > 10^4$$

where the droplet Reynolds number is based on film properties and the relative velocity

$$Re_d = \rho_m\, d\, \Delta U / \mu_m$$

The above equations of motion constitute an initial value problem where the initial values U_d and V_d , d and m_L need to be specified.

III.3 Heat and mass transfer equations for droplets

In the case of a (single component) droplet vaporizing in a gas stream of uniform temperature, the droplet temperature history can be described in terms of a heat-up period, during which the droplet temperature changes,and an 'equilibrium vaporization' period, during which time the droplet temperature remains constant. The physical processes of major significance during these periods are the transport of heat to the droplet and the transport of vapor away from the droplet surface.. The net difference between the energy flux to and away from the droplet accounts for changes in the droplet temperature.

The rigorous mathematical treatment of the droplet vaporization and heating problem requires the solution of time dependent partial differntial equations for the diffusion of mass and energy for conditions both within the droplet and in the surrounding gas phase. Much progress has been made lately in the above area where [Patnaik , 1986] vaporization from a single droplet was considered. Since hundreds of classes of droplets are being considered in a duct where it is not clear if sufficient information is available for calculating the heat and mass transfer coefficients for droplets in forced convection, a simplified approach was used in the present research utilizing the PTRAK code. An existing semi-empirical model [El-Wakil et al., 1954 and Priem and Heidmann, 1960] was extended for use with distillate fuels (or pure compounds) in the PTRAK code.

The following assumptions were made to make the mathematical treatment of the droplet

heat and mass transfer tractable:

(a) At each time t during droplet vaporization and heating, the fluid and thermodynamic conditions of the droplet and gas system adjust instantaneously to steady state conditions (the quasi-steady assumption). The quasi-steady assumption is not an equilibrium assumption.

(b) Conditions within the droplet are uniform. This permits the governing partial differential equations for determining droplet temperature and mass (or diameter) to be reduced to extremely simple forms for quick solution.

(c) Both the droplet and its surrounding are spherically symmetric.

The geometry of the system under consideration is shown in Figure 17 . The droplet is surrounded by a boundary layer of uniform thickness and properties.

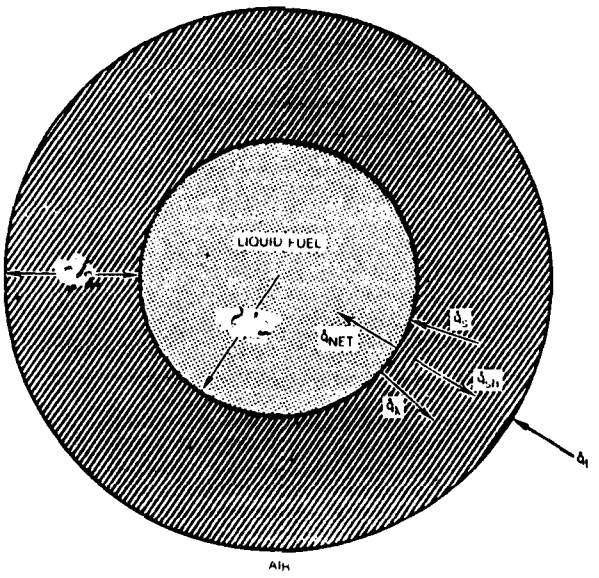

$\dot{q}_{NET}$ — NET HEAT TRANSFER TO LIQUID PHASE
$\dot{q}_s$ — HEAT TRANSFER TO DROPLET SURFACE
$\dot{q}_\lambda$ — HEAT REQUIRED TO VAPORIZE FUEL
$\dot{q}_{sh}$ — SUPERHEAT REQUIRED TO HEAT FUEL VAPOR TO AMBIENT TEMPERATURE
$\dot{q}_l$ — TOTAL HEAT TRANSFER TO SYSTEM

Figure 17. Geometry of droplet vaporization model

At the outer edge of this boundary layer, gas conditions correspond to those of the flow field calculated by the ADD code and will be referred to as the "air" conditions. The equation for droplet vaporization rate is [El wakil et al., 1954]:

$$\overset{o}{w}_L = A_s \bar{k} p_{f,s} \alpha' \qquad \text{(III.4)}$$

where

$$\alpha' = \frac{p_a}{p_{f,s}} \ln\left(\frac{p_a}{p_a - p_{f,s}}\right) \qquad \text{(III.5)}$$

A_S is the droplet surface area, $\tilde{k}$ is the mass transfer coefficient , p_a is the gas phase pressure and $p_{f,S}$ is the vapor pressure at droplet surface at droplet temperature T_L.

The mass transfer coefficient $\tilde{k}$ is obtained from a correlation of the form developed by Ranz and Marshall [1952] for droplet vaprization:

$$Nu_m = \frac{\bar{k}\, d\, T_m\, R}{\Gamma_m M_m} = a + b\, Re_D^{1/2}\ Sc^{1/3} \qquad \text{(III.6)}$$

where Γ_m is the mass diffusivity , M_m is the mean molecular weight of the air-vapor mixture and R is the universal gas constant. The first term on the right hand side expression represents the mass transfer due to free convection while the second term represents the mass transfer due to forced convection. The Schmidt number is defined as:

$$Sc = \mu_m / (\rho_m \Gamma_m)$$

The thermal coefficients used in these parameters are evaluated at a mean boundary layer film condition.

Mean film conditions

At any instant during the evaluation of the vaporization and heating rates, it is assumed that the appropriate properties are constant throughout the film surrounding the droplet. The mean

temperature, T_m, used in the PTRAK code is the log mean value

$$T_m = \frac{T_a - T_L}{\ln(T_a - T_L)} \qquad \text{(III.7)}$$

It is also assumed that the fuel vapor and air thermal coefficients are obtained at a mean fuel vapor concentration (mole fraction):

$$Y_m = 1/2(\, Y_{f,\infty} + Y_{f,s}) \qquad \text{(III.8)}$$

where Y is the fuel vapor concentration at the droplet surface.
The mole fraction is also equal to the ratio of partial pressure to local static pressure so that:

$$Y_{f,\infty} = 0$$
$$Y_{f,s} = p_{f,s}/p_a$$

The mean molecular weight of the mixture at the mean condition is:

$$M_m = Y_m M_f + (1-Y_m)\, M_a \qquad \text{(III.9)}$$

and the mean mass fraction of the fuel vapor is

$$C_m = Y_m M_f / M_a \qquad \text{(III.10)}$$

In addition, the five mean thermal properties that must be evaluated are density, (ρ_m), molecular viscosity (μ_m), thermal conductivity (K_m), heat capacity (C_{pm}) and the diffusion coefficient, Γ_m. From the ideal gas equation of state:

$$\rho_m = p_a\, M_m / (RT_m) \qquad \text{(III.11)}$$

The mean molecular viscosity (μ_m) and the mean thermal conductivity are calculated as mole weighted average quantities. The mean heat capacity is calculated as

$$C_{pm} = C_m C_{pf} + (1 - C_m) C_{pa} \qquad \text{(III.12)}$$

where the heat capacities C_{pf} and C_{pa} are evaluated at T_m.

The diffusion coefficient Γ_m is estimated as suggested by El Wakil [1954] using the kinetic theory result [Hirschfelder et al., 1954]. Force constants for Jet-A fuel are as given by Anderson et al [1982]. Force constants for water (as the liquid phase) and air were obtained from standard references

Droplet heat transfer

The droplet heating rate equation is

$$\frac{dT_L}{dt} = \frac{\overset{o}{q}_s - \overset{o}{w}_L \lambda}{\frac{\Pi}{6} d^3 \rho_L C_{PL}} \qquad \text{(III.13)}$$

where the total amount of heat arriving at the droplet surface is

$$\overset{o}{q}_s = h A_s (T_a - T_L) \, z / (e^z - 1) \qquad \text{(III.14)}$$

and the parameter z is

$$z = \frac{\overset{o}{w}_L C_{pf}}{h A_s} \qquad \text{(III.15)}$$

$\overset{o}{w}_L$ is the liquid fuel vaporization rate and λ is the heat of vaporization. The droplet surface area A_s is calculated from:

$$A_s = \pi d^2$$

The above equation is the product of the forced convection heat transfer rate for a nonvaporizing

system $h A_S (T_a - T_L)$, and a correction term for the energy carried away from the droplet due to mass transfer (i.e., "blowing" of the boundary layer), $z / (e^z - 1)$. This term approaches unity for a zero mass transfer rate and zero for an infinite mass transfer rate (no energy reaching the droplet surface).

The heat transfer coefficient h is obtained from a correlation (similar to that used for the mass transfer coefficient) developed by Ranz and Marshall [1954]:

$$Nu_h = \frac{h d}{K_m} = a' + b' Re_a^{1/2} Pr^{1/3} \qquad (III.16)$$

where the Prandtl number is defined as

$$Pr = \mu_m C_{pm} / K_m$$

For reasons similar to those presented during the discussion of the mass transfer coefficient, the coefficients a' and b' are assigned the values:

$$a' = 2.0$$
$$b' = 0.6$$

Some of the heat arriving at the droplet surface is used to vaporize an amount of fuel, $\dot{w}_L$ while the remainder is used to heat the droplet. At equilibrium, $\dot{q}_S$ is equal to $\dot{w}_L \lambda$ and the droplet temperature (the wet bulb temperature) is constant (for a pure fluid).

At any instant, the droplet mass is given by

$$m_L = \frac{\Pi}{6} d^3 \rho_L \qquad (III.17)$$

Since

$$\frac{dm_L}{dt} = - \dot{w}_L \qquad (III.18)$$

the equation for the rate of change of droplet diameter is given as

$$\frac{d(d)}{dt} = -\frac{2}{\Pi d^2 \rho_L}\left[\overset{o}{w}_L + \frac{\Pi d^3}{6}\frac{d\rho_L}{dT_L}\frac{dT_L}{dt} \right] \qquad \text{(III.19)}$$

Fuel properties required in the model

Both liquid phase and vapor phase properties are required in the droplet evaporation calculations. The fuel vapor molecular viscosity (μ_f), the thermal conductivity (K_f) and the heat capacity (C_{pf}) are obtained (as function of the mean film temperature) from polynomial expressions.

For distillate fuels, the vapor pressure ($p_{f,s}$) is evaluated using Cox's procedure [1923]. A distillate fuel is a liquid mixture consisting of two or more compounds that may differ chemically and physically. For a pure substance, such as water or a single hydrocarbon compound, the vapor pressure is a function of only the temperature of the liquid. For a distillate, it is not practical from a computational standpoint to keep track of each component and calculate its contribution to the vapor pressure. In Cox's method it is assumed that at any instant during the vaporizing process, the behavior of the distillate fuel is the same as that of some pure substance; that is its vapor pressure is a function of the liquid temperature only. Different pure substances characterize the vaporization process at each instant. Further details of application of the above procedure to the PTRAK code can be found in Anderson et al. [1982].

The liquid density (ρ_L) and heat capacity (C_{pL}) are calculated from polynomial expressions (as a function of liquid temperature). The liquid molecular viscosity (μ_L) is determined from:

$$\ln \mu_L = \sum_{N=1}^{4} A_N \, T^{N-1} \qquad \text{(III.20)}$$

where A_N are the polynomial coefficients

Finally, the heat of vaporization (λ) is calculated using the Clausius-Clapeyron equation which relates λ to the slope of the vapor pressure curve:

$$\frac{d\,(\ln p_{f,s})}{dt} = \frac{-\lambda M_f}{R\,T_L^2} \qquad \text{(III.21)}$$

III.4 Droplet class and distribution functions

For the present calculations employing the PTRAK code, the state of a droplet at any instant of time is uniquely determined by its location (x, y), velocity (U_d , V_d) in space, its diameter (d) and its temperature (T_L). In principle it is is possible to solve this set of equations for each of the individual droplets. However, the number of droplets to be considered can be substantially reduced by treating each droplet as though it were a cloud of 'n' fuel droplets, the mean properties of which are equal to the properties of the individual droplet.

A droplet class is defined in the Lagrangian sense by specifying the number of droplets n_I which are within given bounds of location, velocity, droplet diameter and temperature at time = 0. In the absence of droplet collisions, the number of droplet classes in phase space at any given time determines the state of the entire cloud of droplets. The fuel flow rate is thus given as

$$\Omega_L = \sum_{I=0}^{IN} n_I \, m_I \qquad \text{(III.22)}$$

Two distribution functions (the binomial and the Rosin-Rammler) were employed to characterize the droplet sizes at the inlet. For the binomial distribution function, the mean particle diameter and the particle variance (standard deviation) need to be specified along with the number of size classes. The binomial distribution function is given as

$$f_B(I) = \frac{(IL)!}{I!\,(IL - I)!} \left(\frac{1}{2}\right)^{IL}, \quad I = 0, IL \qquad \text{(III.23)}$$

where IL is the number of size classes. Also

$$\sum_{I=0}^{IL} f_B(I) = 1.0 \qquad \text{(III.24)}$$

As IL $\rightarrow \infty$, the binomial distribution function approaches the normal (Gaussian) distribution function.

The Rosin - Rammler distribution function is more commonly used to characterize the droplet size distribution typically produced by gas turbine fuel injectors. The Sauter mean diameter (SMD) of the spray , the width factor m and the number of size classes have to be specified for the above distribution function. The mean droplet size can be uniquely determined if the SMD and the width factor for the spray is specified.The width factor provides a measure of the spread of the drop sizes. The higher the value of m, the more uniform is the spray. If m is infinite, the drops in the spray are all the same size. For most fuel sprays, the value of m lies between 2 and 4. For airblast atomizers, Simmons [1977] quotes a value of 2.59. In the present calculations, the value of m was set equal to 3.46.

III.5 Numerical Methods

The equations of motion for the droplets along with the differential equations for droplet diameter and temperature are solved as an initial value problem using a predictor corrector method which is second order accurate in Δt. The length of the duct is divided into stations (usually finer than the division used in the ADD code) and the initial guess for the variables at station I + 1 are the corresponding values at station I. The differential equations are then evaluated at the mid point. The equations are solved for the unknown time (required for the droplets to arrive from one station to the next) in an iterative manner.

Depending on the number of total classes (N) of droplets (product of the droplet classes based on initial diameter, velocity, location and temperature), N sets of equations of motion along with the differential equations of droplet size class temperature and droplet size class diameter are solved in a forward marching procedure.

III.6 Results and discussion

The fuel evaporation effects in a square duct were studied where the fuel is injected from the end of an airblast atomizer located at the tip of the splitter plate (see Figure 2). The PTRAK code was employed (in conjunction with the ADD code) for this purpose.Droplet shattering and coalescence were not considered in the present study.

Air velocities at the exit plane of the atomizer are nonuniform and hence a turbulent shear layer forms downstream .The flow field in the square duct is calculated first with the modified ADD code using a k -ϵ turbulence model. Calculations of the nonequilibrium heating and vaporization of the fuel droplets are then carried out using the gas flow solution obtained first. In this case , direct comparisons of the predicted results were not possible due to the lack of corresponding measurements in the parallel experimental work. However, qualitative comparisons of the predictions and the laser diffraction measurements of the water droplets in the tunnel were in agreement.

In this section, results obtained with the unmodified PTRAK code (employing a deterministic separated flow model) are presented. Finite transport rates are considered so that the fuel droplet behavior is affected by the airflow behavior. The fuel spray at the exit of the atomizer is characterized either by the binomial or the Rosin-Rammler distribution function. The spray is described by the behavior of a number of droplet classes, each having a different initial state regarding the diameter, temperature, velocity relative to the gas stream and spatial location.

The predictions of two sets of calculations are reported below. In the first set, Jet - A (multi-component) fuel was considered as the liquid phase and the binomial distribution function was used to characterize the spray at the exit of the airblast atomizer. In the second set, a water spray was considered which was characterized by a Rosin-Rammler distribution. It is noted that for the experimental measurements in the parallel experimental program, water was atomized and sprayed in the duct.

For the first case, uniform air velocities of 60 m/s (U_{afs}) and 30 m/s (U_{aas}) were considered on the two sides of the splitter plate. In order to study the effects of air flow field characteristics on Jet-A fuel evaporation, two sets of inlet static pressure and stagnation temperature

values (5 atm. , 400 K and 10 atm. and 750 K) were considered for the air flow. A duct length of 2.5 cm. was considered for the computation of the two dimensional flow field. Insulated walls were considered for the duct. For the Jet-A fuel, the 90% distillation temperature at 1 atm. was considered to be 524 K [Anderson et al., 1982]. A 50 x 40 (x x y) grid was considered for the computation of the gas flow field. For the lower pressure -temperature (5 atm., 400 K) gas flow field, the Reynolds number (based on the width of the duct and the average inlet velocity [U_{afs} + U_{aas}]/2) was 4.7 x 10^7. The gas flow field predictions are similar to those presented in an earlier chapter. The results show the development of a shear layer and at larger values of the downstream location, the flow becomes essentially self-similar.

The Jet-A fuel thermophysical properties are given in Anderson et al. [1982]. Binomial size distribution of the droplet classes were considered for the calculations. The mean droplet size of the spray was specified and the standard deviation was set equal to zero. This, in effect reduced the spray to a monodispersed spray. The fuel droplets were divided into ten classes (based upon the injection angle and inlet velocity componenets) between 30° and 50° and -30° and -50° .The angles are measured from the horizontal axis, with the anti-clockwise direction being positive. Each class was assigned the same initial temperature. The droplets were assumed to have an inlet velocity of 30 m/sec. The total fuel flow rate was kept at 0.015 kg/sec to ensure the low equivalence ratios necessary for the assumptions in the formulation of the problem.

The results of these calculations can be found in Farouk et al. [1987] and are not repeated here. The purpose of these calculations were to essentially demonstrate the predictive abilities of the PTRAK code in the two dimensional duct situation.

In the second case water was considered as the dispersed phase. For predictions of droplet trajectory and evaporation characteristics, the gas flow field solution was first obtained with U_{afs} = 91.4 m/sec and U_{aas} = 45 m/sec. The inlet gas temperature was maintained at 400 K and the pressure was set equal to 1 atm. The initial conditions for the gas phase computations were obtained from measurements . The agreement of the experimental and computational results of the mean velocity and turbulent intensity at downstream locations was reasonable.

Water spray evporation was then considered in the above flow field. The spray was

characterized at the inlet by the Rosin-Rammler distribution function. The initial SMD of the spray was considered to be 91 μm and the spray was divided into eleven size classes. The width factor of the Rosin-Rammler distribution was set equal to 3.46. To realistically simulate the conditions at the exit of the prefilming atomizer, six trajectories were considered (± 1° to ± 9° with increments of 4°) for the spray. The eleven size classes were considered for each trajectory. Hence sixty six sets of droplet trajectory, diameter and temperature equations were considered for the solution. Each class was assigned a small initial velocity (0.1 m/sec) and the initial droplet temperatures were set equal to 350° K.The total liquid flow rate was maintained at 0.015 kg/sec. The above parameters for the spray were similar to the conditions realized in the parallel experiments.

The calculations were carried out for a duct length of 25 cm (measured from the exit plane of the atomizer/splitter plate). For the length of the computational domain and the temperatures of the gas flow and the incoming droplets, the evaporation predicted was insignificant. Similar observations were also made in the experimental studies. Significant evaporation of the water droplets were observed if the gas flow was only at higher pressures and temperatures. However, those values of pressure and temperature could not be attained in the experimental facilities developed. The droplet velocities and temperatures, were also not measured in the parallel experiments.

Figure 18 shows the streamwise velocities of the largest (240 μm), smallest (20 μm) and the intermediate (105 μm) size class droplets injected at 1° (towards the high velocity side) as a function of time. The smallest size class attains the gas flow velocity within a short time and exits the computational domain earlier than the larger size classes. The intermediate and the largest size class droplets exhibit significant slip between their velocities and the gas phase velocity (U_{afs} = 91.4 for this case). The temperatures histories of the above three classes (injected at 1°) are shown in Figure 19 . For all three classes, droplet temperature was found to drop due to evaporation . For the larger two size classes, the temperature drops monotonically, whereas for the smallest size class droplet it is found that due to reduced evaporation, at one point, the convective heat transfer from the hot the gases overtakes the cooling due to evaporation . Similar observations were made for other size classes in the other trajectories considered. Due to the lower velocities of the gas phase flow encountered by trajectories at - 1° through - 9°, longer residence times of the

droplets size classes were encountered.

The calculations were also repeated for a different initial droplet temperature (314° K) while all other parameters remained as above for the gas and liquid phases [Farouk et al. , 1987b]

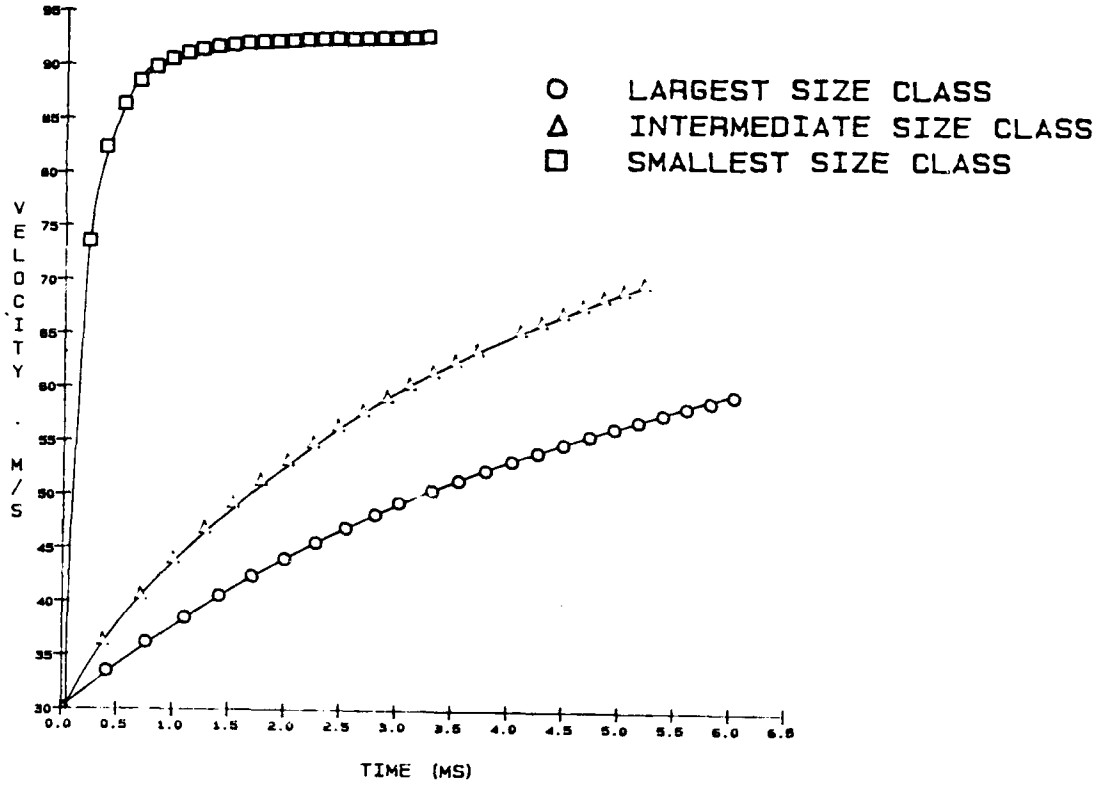

Figure 18. Streamwise droplet size class velocities for trajectories at 1° angle.

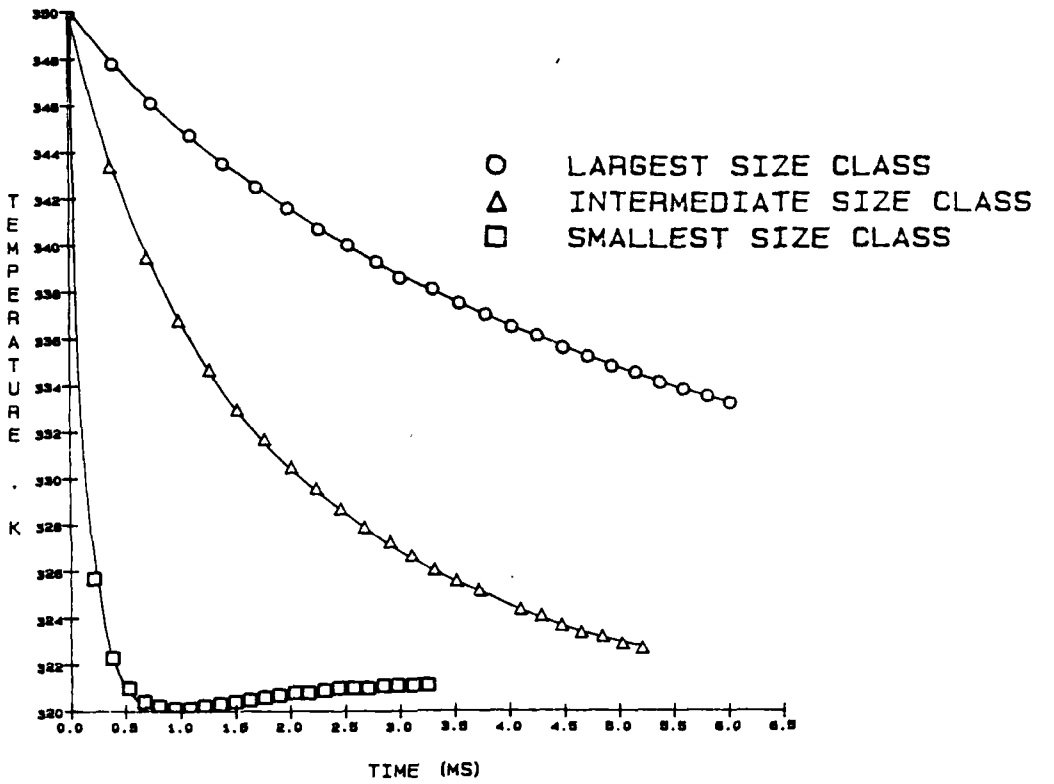

Figure 19. Droplet size class temperatures for trajectories at 1° angle.

1987b). The results indicated that the amount of evaporation for the droplets was further reduced and from the very beginning all size classes showed an increase of temperature .

Due to the absence of the normal component of the gas phase velocity (V = 0.0) in the ADD code predictions and the deterministic separated flow model employed in the PTRAK code, the prediction of the droplet size class trajectories become entirely dependent on the initial droplet velocity and initial trajectory angle. Both of these parameters need to be determined experimentally for the prefilming airblast atomizer.

IV. ANALYSIS OF DROPLET BEHAVIOR - STOCHASTIC MODEL

IV. 1 Background and general approach

Recent models for dilute, particle-laden jets differ in details, but generally may be divided into two main categories [Shuen, 1984]: (1) locally homogeneous flow (LHF) models, where infinitely fast interphase transport rates are assumed; (2) separated flow (SF) models, where finite interphase transport rates are considered.

In the Locally Homogeneous Flow (LHF) models the slip between the phases is neglected. The main assumption of LHF models is that interphase transport rates are fast in comparison to the rate of development of the flow as a whole. This implies that all phases have the same velocity and temperature and that phase equilibrium is maintianed at each point in the flow, i.e.,the flow is locally in thermodynamic equilibrium. LHF models are only correct when the dispersed phase has infinitely small particle sizes.

Faeth and his coworkers studied evaporating and combusting sprays [Faeth, 1979, 1980], and condensable vapor or gas jets in liquid using LHF models. It was found that while LHF models provide a reasonable first estimation of the structure of these processes, they generally overestimate the rate of development of the flow. For their experimental conditions, a spray having a Sauter mean diameter (SMD) smaller than 10μm would be required for quantitative accuracy of the LHF model. However, it was indicated that LHF models still have some advantages [Faeth, 1979], namely,

(1) they require minimal information concerning initial conditions of particle properties and particle sizes - properties which are often difficult to obtain for practical flows;

(2) the theoretical model of the flow is equivalent to that of a single-phase flow and effects of multiple phases only appear in the representation of state relationships (thermodynamic properties and molecular properties), bypassing the difficulties involved with modeling interactions between the phases; and

(3) LHF models involve less empiricism than the SF models.

Recent models of dilute particulate flows have mainly employed the discrete particle

formulations. These formulations generally follow an approach called "particle-source-in-cell" (PSIC) model [Crowe, 1977]. This involves dividing the discrete phase into representative samples whose motion and transport are tracked through the flow field using a Lagrangian formualtion. The samples of the discrete phase are chosen to provide a statistically significant representation of the process. An Eulerian formulation is generally employed to solve the governing equations for the continuous phase, similar to the solution of the flow equations for LHF
models. The effects of interphase transport is considered by introducing appropriate source terms in the governing equations for the continuous phase - determined from the particle tracking computations. Most discrete particle models apply the dilute flow approximation, i.e., particle collisions, effects of nearby particles on particle transport rates, and the volume occupied by particles are usually ignored.

Deterministic Separated Flow (DSF) models adopt the discrete particle formulation neglecting effects of turbulence on interphase transport properties and the dispersion of particles by turbulent fluctuations. The solution method employed in the PTRAK code falls under this category. Neglecting turbulent particle dispersion is appropriate when characteristic particle response times are large in comparison to characteristic times of turbulent fluctuations. However, few practical flows satisfy this requirement. Even when modified to account for particle dispersion, DSF models incur errors when the mean properties of the continuous phase are used to evaluate interphase transport rates [Faeth, 1983]. Earlier work has shown that these errors are particularly significant during the evaluation of particle drag.

In the Stochastic Separated Flow (SSF) models, effects of interphase slip and turbulent dispersion are considered using random sampling for gas phase turbulence properties in conjunction with random-walk computations for particle motion using Monte Carlo methods [Gosman and Ionnides, 1984; Shuen, 1984]. Most practical particle-laden flows exhibit properties which require consideration of turbulent dispersion. Several recent studies of turbulent drop dispersion use SSF model which have given promising results. Turbulent dispersion of drops has generally been neglected in past separated flow models of sprays. Neglecting dispersion implies that drops follow deterministic trajectories prescribed by their initial condition at the injector exit and mean gas properties throughout the flow field. In locally homogeneous flow models , on the other hand, drops disperse due to turbulence at the same rate as the gas phase. Actual behavior lies between these two limits, depending on the inertial properties of the drops and the turbulence properties of the gas phase. Techniques for treating turbulent dispersion are rapidly developing and some representative methods are discussed in the following.

Two main methods have been employed to compute particle dispersion in sprays. The earliest investigations modeled turbulent dispersion using a gradient diffusion expression which employs a turbulent gas/particle exchange coefficient. Some method of estimating the gas/particle turbulent exchange coefficient is required. Hinze [1975] reviews theoretical and experimental studies of gas/particle exchange coefficients. Existing continuum analysis for gas/particle exchange coefficients has a limited range of application, since the process must be substantially simplified in order to obtain closed form solutions [Hinze, 1975]. The main difficulty is that dispersion is influenced by both particle and turbulence properties, adding a whole new dimension to the problem of estimating a turbulent exchange coefficient. Lack of theoretical guidance on values of gas/particle exchange coefficient is compounded by difficulties with existing measurements. These requirements are rarely satisfied in practice. Even in cases where the experiments were properly analyzed, it is unlikely that the results could be directly applied to a particular fuel spray since both particle and turbulence properties must be the same, because both sets of characteristics influence dispersion properties. Gradient diffusion models of particle dispersion are not particularly convenient for incorporation in the Langrangian particle motion calculatins. Jurewicz and Stock [1976] proposes circumventing this problem by representing the effects of particle diffusion as an effective drift velocity which is found from the gradient diffusion expression [Jurewicz, 1976]. Unfortunately, this introduces errors due to numerical diffusion which compromises one of the advantages of the Lagrangian formulation.

Another melthod is proposed for employing estimated turbulent gas/particle exchange coefficients to compute particle dispersion [Hotchkiss, 1972, Dukowicz, 1980]. In this case, the turbulent exchange coefficient is related to the variance of the probability density function of particle position (assumed to be Gaussian) at the end of each computational time step. Given the variance, the distribution is randomly sampled to obtain the diffusional increment of particle position. This procedure does not provide any real advantages over the stochastic methods [Gosman and Ionnides, 1983], unless the exchange coefficient can be prescribed very simply. The method has not been applied to separated flow computations for sprays.

Recent analysis of particle dispersion in sprays have employed stochastic methods which model particle dispersion directly. A turbulence model provides the instantaneous properties of the environment of a particle during a Lagrangian computation of particle motion. This involves random sampling to determine gas flow properties in addition to considering a representative number of particle trajectories. Past computations with stochastic particle dispersion models have

used a variety of turbulence models. The main features of the stochastic dispersion model of Gosman and Ioannides [1983] are discussed in the following. This method employs a $k - \varepsilon$ turbulence model and is easily adapted for use in most "discrete droplet models" of sprays. Furthermore, this model has been employed to estimate the effect of dispersion in evaporating and combusting sprays, yeilding resutls of some importance to spray modeling.

Gosman and Ioannides compute the motion of a particle using the Lagrangian formulation. For particle dispersion calculations, the instantaneous gas velocities replaces the mean velocities in the governing equations. As particles pass through the flow, they are assumed to interact with individual eddies. Flow properties within each eddy are assumed to be constant. Each interaction deflects the particle as dictated by the instantaneous eddy velocity. Therefore, the particle trajectory is determined similar to a random walk computation until the particle passes out of the region under consideration. Overall particle behavior is obtained by averaging over a statistically significant number of independent calculations .

IV.2 Mathematical model

The above stocahstic model [Gosman and Ioannides , 1983] for droplet dispersion has been considered in the present research for the prediction of evaparating sprays in a confined shear layer. Significant modifications to the PTRAK code has been done to achieve this goal. The instantaneous gas velocity within an eddy (at a given location) is obtained from the mean gas velocity and the turbulent kinetic energy k, which are known from the solution of the governing equations of the gas phase (using the ADD code). The turbulence is assumed to be isotropic with fluctuating components having a Gaussian distribution for this computation. The standard deviation of the distribution is taken to be $(2k/3)^{1/2}$. The distribution is randomly sampled when a particle enters an eddy to obtain the instantaneous velocities as

$$U = u + u' \text{ and } V = 0 + u'$$

A particle is assumed to interact with an eddy for a time taken as the smaller of either the eddy lifetime, t_e, or the transit time, t_t, required for the particle to traverse the eddy. The eddy lifetime and transit times are determined by assuming that the characteristic size of the randomly sampled eddy is the dissipation length scale, L_e, given by

$$L_e = C_\mu^{3/4} k^{3/2} / \varepsilon \qquad \text{(IV. 1)}$$

The eddy lifetime is then estimated as

$$t_e = L_e / |u'| \qquad \text{(IV.2)}$$

The droplet transit time is determined from the following equation

$$t_t = -\tau \ln [1 - L_e / (|u - U_d|)] \qquad \text{(IV.3)}$$

where τ is the particle relaxation time

$$\tau = 4/3 \, \rho_f d / (C_d |u - U_d|) \qquad \text{(IV.4)}$$

IV. 3 Modifications to the PTRAK code

The stochastic separated flow (SSF) model involves finding trajectories and evaporating characteristics of individual particles (using a statistically significant number of independent calculations) as they move away from the injector and encounter a random distribution of turbulent eddies.

Key elements in the SSF model are the method used to specify eddy properties and the time of interaction of a particular eddy. An approach is proposed to use direct simualtion of these properties [Shuen, 1984]. Properties are assumed to be uniform within each eddy and to change randomly from one eddy to the next. Particle trajectory computation method is the same as that given in the PTRAK code, however, mean-gas properties in the particle equations are replaced by the instantaneous properties of each eddy.

The properties of each eddy are found at the start of particle-eddy interaction by making a *random selection from the probability density function* (PDF) of velocity. Velocity fluctuaitons are assumed to be isotropic with a Gaussian PDF having a standard deviation of $(2k/3)^{1/2}$ and mean components of U and zero in the x and y directions respectively. Considering zero mean component of velocity in the y direction is the result of using simplifying assumptions in the ADD

code. The cummulative distribution function for each velocity component at a given location is constructed and sampled. This involves randomly selecting a number in the range 0 - 1 and computing the instantaneous velocity components from the cummulative distribution function. This procedure provides a random selection of eddy properties which satisfies the PDF for velocity fluctuations.

For implementing the stochastic separated flow model, we need to randomly select the instantaneous velocity, u, at a point in space (recall that $u = U + u'$).

Since we have assumed that the velocity distribution function is Gaussian, the probabilty density function of the velocity is given as

$$p(u) = \frac{1}{\sigma\sqrt{2\pi}} \exp\left[\frac{-(u - a)^2}{2\sigma^2}\right] \qquad (IV.4)$$

where a is the mean and σ is the standard distribution.

If we construct the cumulative distribution function of u, all the possible values of u will be in the range of $0 < p(u) < 1$. . A random number generator will generate a value between 0 and 1, say A $(0 < A < 1)$, which corresponds to

$$\int_0^{u(A)} p(u)\, du = A \qquad (IV.5)$$

or

$$\int_0^{u(A)} \frac{1}{\sigma\sqrt{2\pi}} \exp\left[\frac{-(u - a)^2}{2\sigma^2}\right] du = A \qquad (IV.6)$$

With the known mean quantity 'a' and the standard deviation σ, p(u) is uniquely defined and A is given by the random number generator. The only unknown in the above equation is the upper limit u(A) which can be solved by numerical integration melthods. Consequently we can randomly

simulate the instantaneous velocity u at any point in space.

The equations of motion for the fuel droplet trajectories presently coded into the PTRAK computer program are given in an earlier section. U_d and V_d are the mean droplet velocities in the streamwise and normal coordinates respectively. The instantaneous droplet velocities (as calculated in each indepenedent calculation with the stochastic model) is given by

$$u_d = U_d + u_d'$$

and

$$v_d = V_d + v_{d'}$$

where the mean droplet velocities are obtained by averaging a statistically significant number of realizations.

Summarizing, the following procedure is adopted to implement the stochstic separated flow model in the ADD and the PTRAK codes:

a. The solutions for the turbulent kinetic energy (k) and the dissipation rate (ε) as obtained by the ADD code are stored in a data file which is subsequently read by the PTRAK code.

b. Depending on the droplet size classlocation in the flow field, the corresponding values of the turbulent kinetic energy and the length scale L_e are calculated by interpolation.

c. With the mean gas velocities and the standard deviation known at the droplet size class location, the instantaneous gas velocities are obtained by selecting a random number via a random number generator.

d. For droplet trajectory and evapration characteristics calculations, the mean gas velocities are replaced by the instantaneous gas velocities.

e. When the droplets arrive at the next sub-station, the time required for the flight is compared with t_e and t_t. If the droplet travel time is larger than any of t_e and t_t, step 'c' is repeated for the new droplet location. This procedure is continued till the droplets exit the computational domain.

f. Statistically significant number of independent calculations are performed. From them ,

averaged values of U_d, V_d, droplet diameter class, droplet temperature etc. are computed along the length of the duct.

IV.4 Results and discussion

The modified PTRAK code along with the gas flow predictions by the ADD code can be employed to predict the spray evaporation characteristics in the turbulent duct flow. The effect of the gas phase turbulence on droplet dispersion is considered via a stochastic separated flow model. The amount of droplet evaporation in the parallel experiments was found to be insignificant for the gas flow pressure and temperatures in the duct and the water temperature at the atomizer. Since the predictions for the stochastic separated flow model were obtained for conditions similar to those in the experiments, the droplet evaporation within the 25 cm of the duct length considered was small. The dispersion effects of the droplet size classes were only of significance. The changes due to gas phase turbulence on the droplet temperature history and the evaporation rate was minimal, for the operating conditions studied.

A wake flow field was considered for gas phase computations where U_{afs} and U_{aas} were both set equal to 91.4 m/sec. The inlet values for the mean axial velocity was obtained from experimental measurements at x/D = 0.03. The pressure and temperature of the gas flow field at the inlet was uniform and was set to 1 atm. and 400 K respectively. Due to the presence of the splitter plate, a turbulent wake flow is created downstream. The mean axial flow solution, U(x,y) along with the turbulent kinetic energy and dissipation rate solutions, k(x,y) and ε(x,y) were stored and subsequently read by the PTRAK code. Water was considered as the dispersed phase and a Rosin-Rammler distribution function was employed to characterize the spray at the tip of the airblast atomizer. The spray was divided into eleven size classes with SMD = 120μm and the width factor of 3.46. In order to investigate the dispersion characteristics of the spray, only one trajectory of the spray was considered with an injection angle of 1°. Each class was assigned the same initial temperature of 314 K. Though only one trajectory was considered, the fuel flow rate was still maintained at to 0.015kg/sec. For the initial velocity of the droplet size classes, several cases were investigated. It was observed that the dispersion effects due to gas phase turbulence diminshes with increasing inlet velocities of the droplets. Figure 20 shows the trajectories of the smallest (24 μm) the largest (340 μm) and the intermediate size (210 μm) classes using the unmodified PTRAK code. The initial droplet velocity was set equal to 10 m/sec. No effect of the gas phase turbulence is accounted for in this result. The smallest size class exits the computational domain first and is strongly influenced by the parallel (axial) gas flow field. The larger size classes (due to the initial

injection angle and larger inertia) continue to move obliquely in the parallel gas flow field.

The modified PTRAK code (with a stochastic separated flow model) was then applied to calculate the trajectories and evaporation characteristics of the above size classes with identical initial conditions. A statistically significant number of independent computer runs were made where the instantaneous gas flow field at any location (u = U + u' and v = 0 + u') was simulated by procedures described earlier. The stored values of the turbulent kinetic energy was used to compute the vallues of u' at any droplet location. The stored values of the the dissipation rate of turbulence was used to compute the eddy lifetime t_e and the droplet transit time t_t as described earlier. Figures 21, 22 and 23 show the droplet size class trajectories for three independent calculaions performed by the modified PTRAK code. Comparing these results with Fig. 20 (obtained by using the unmodified PTRAK code), the efects of the gas phase turbulence on the droplet trajectories is evident. As expected, the effects are stronger for the smallest size droplets. Due to the stochastic approach used, the results in Figs. 21, 22 and 23 vary in details, but qualitatively exhibit the same behavior. A 'statistically significant' number of these computations (realizations) were obtained and then the solutions were averaged . Figure 24 shows the predicted trajectories of the droplet classes after the averaging process.

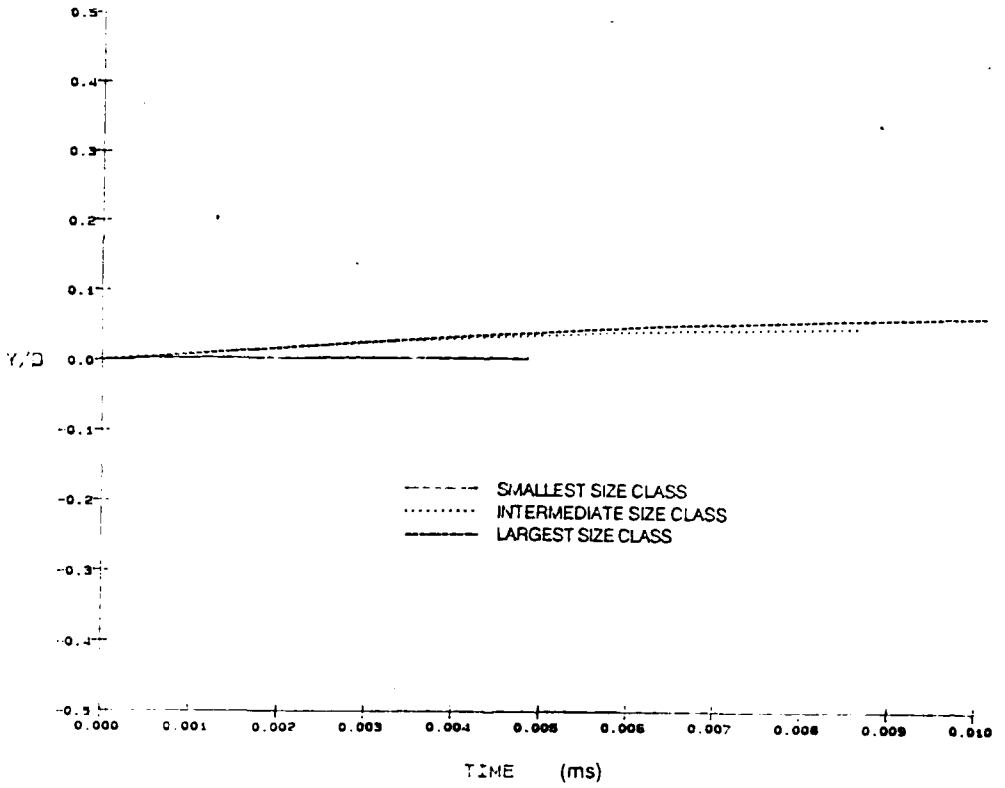

Figure 20. Droplet size class trajectories obtained with the unmodified PTRAK code.

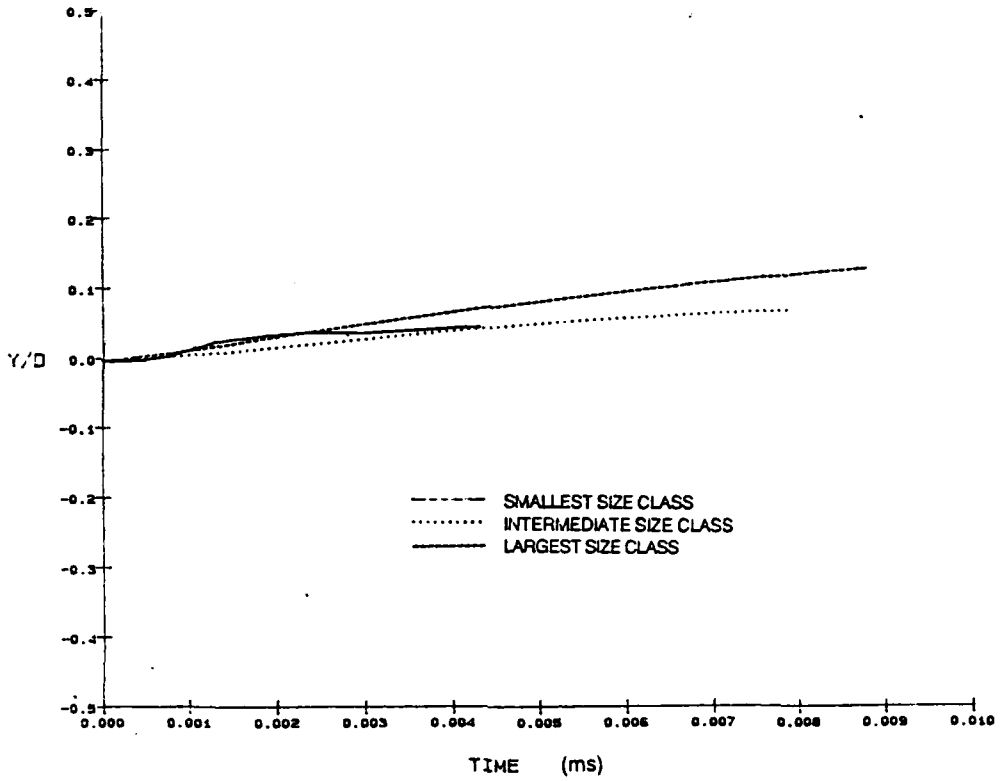

Figure 21. A realization of the droplet size class trajectories obtained with the modified PTRAK code .

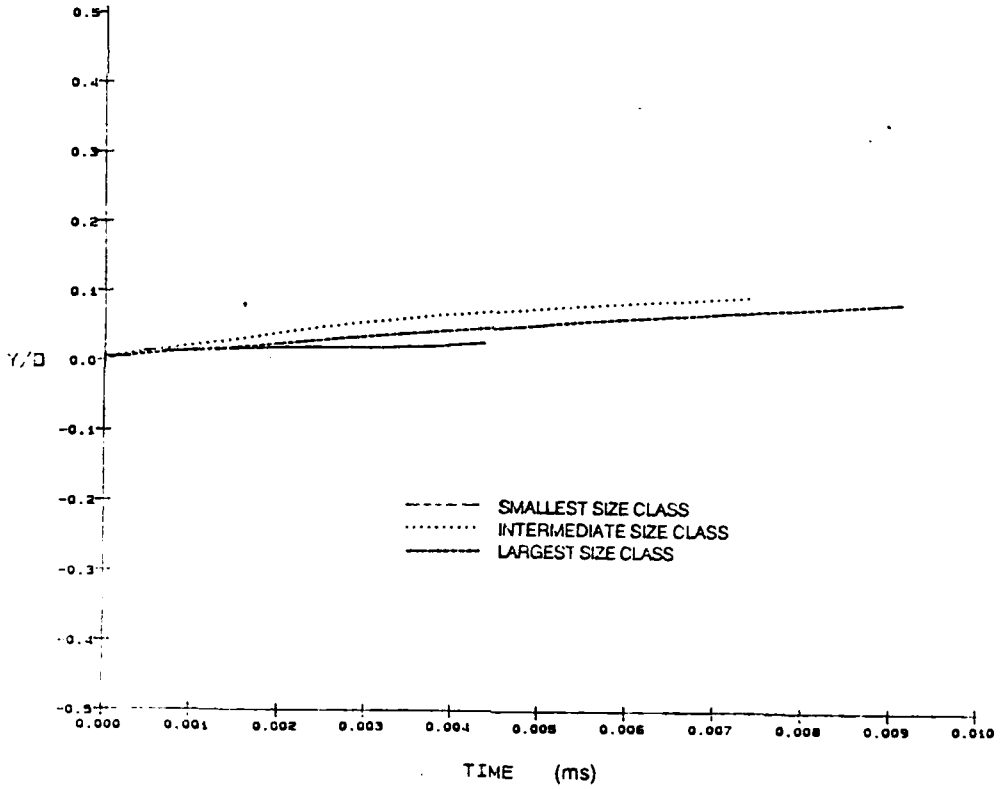

Figure 22. A realization of the droplet size class trajectories obtained with the modified PTRAK code .

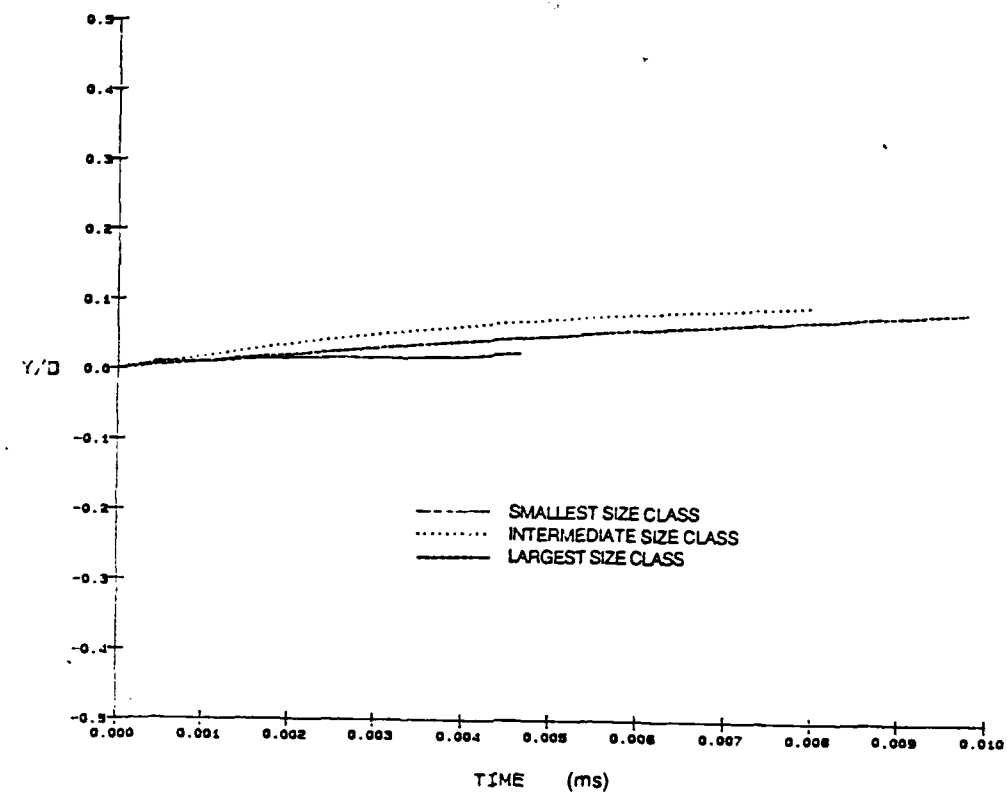

Figure 23. A realization of the droplet size class trajectories obtained with the modified PTRAK code .

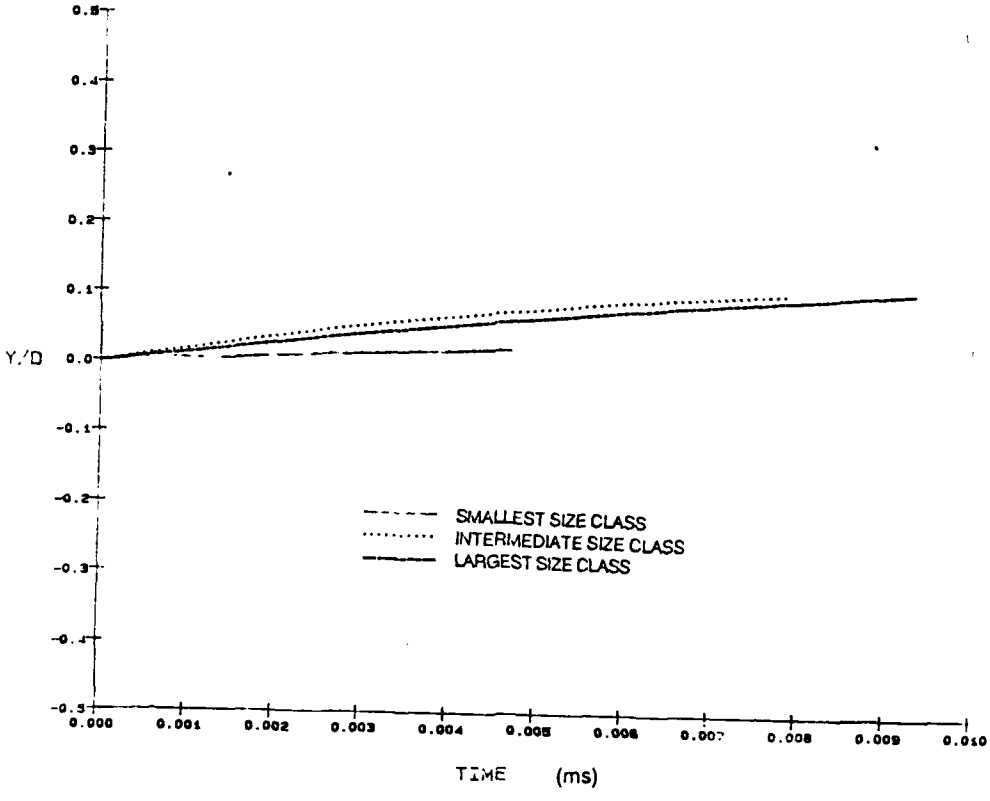

Figure 24. Droplet size class trajectories (averaged) obtained with the modified PTRAK code .

Comparing Figures 20 and 24, it seen that at the exit of the computational domair, the smalles size class droplet is deflected (in the nor,mal direction) the highest amont due to the gas phase turbulence (about 135% more than he predictions obtained with the deterministic separated flow model). For the intermediate and the largest size classes the effects were less pronounced, but significant (80% and 45% more deflection in the normal direction). Similar behavior of the spray was observed for the spray in the experimental studies. Droplet size class temperature and evaporation predictions with the stochastic separated flow model did not show significant variations with those obtained with the unmodified PTRAK code for the flow and initial droplet size conditions considered. These are primarily due to the low temperature difference between the gas phase flow and the initial liquid temperatures. In a gas turbine air-fuel passage, the air is at higher pressure which enhances fuel evaporation. The effects of droplet dispersion can be studied more effectively with the modified PTRAK code if the appropriate gas flow field conditions are used in the simulations.

V. SUMMARY AND CONCLUSIONS

A computational study was undertaken to study the evaporation characteristics of a liquid spray in a confined turbulent shear flow. The computations modeled parallel experiments carried out under ARO sponsorship (Grant No. DAAG29-84-K-0165). The experiments were carried out in a vertically down-flowing wind tunnel where a splitter plate separates two air streams whose average velocities can be controlled independently. Depending upon the values of the avearge velocities on each side of the splitter plate, a turbulent shear layer or wake flow develops at the end of the splitter plate in the duct.. A flat prefilming airblast atomizer is located at the tip of the splitter plate. The trajectories and the evaporation characteristics of the water spray formed at the atomizer are affected by the turbulent gas phase flow field. The droplet formation process is also affected by the flow characteristics on the two sides of the splitter plate.

The computer codes ADD and PTRAK [Anderson et al., 1982] developed for the prediction of flow field and fuel evaporation characteristics in prevaporizing-premixing fuel air passages (of gas turbine combustors) were chosen for carrying out the computations. This was perhaps a poor choice due to the complexities of the turbulent flow field in the experimental configuration and the spray formation process in the airblast atomizer. The flow situations considered in the present research program are considerably more complicated than the axisymmetric parabolic duct flow situations that are suitable for the ADD and the PTRAK codes. In fact, the flow field within a gas turbine combustor (dominated by strong shear layers) are inherently more complex than those found in axisymmetric ducts. Extensive modifications to the ADD code had to be performed to obtain predictions for the two dimensional turbulent shear flows (at the end of a splitter plate located along the axis of the duct) which agreed reasonably well with the measurements.

The normal component of the mean gas velocity is not solved by the ADD code (due to the orthogonal streamline coordinate system employed). Neither can it handle significant flow reversal. These introduce errors in calculating flow fields at the exit of the splitter plate. Due to the parabolic formulation, it was also not possible to include the splitter plate in the computational domain. Recent studies have shown that considering the splitter palte within the computational domain significantly enhances the accuracy of the shear layer predictions [Grinstein et al., 1986]. Current efforts are underway at Drexel University to compute the flow field in the experimental tunnel using an elliptic formulation of the governing equations. Efforts in tuning the parameters of the k -ε

model for the gas phase turbulence produced some improvements in the predictions.

The ADD and PTRAK codes suffer from another major limitation in the formulation, i.e. there is only one way coupling between the gas phase and the dispersed phase computations. The effect of droplet evaporation is not considered in the gas flow computations. This assumption is reasonable for computations in a long prevaporizing-premixing duct. However, for computations close to an atomizer in a combustion chamber, this can introduce significant errors.

The computations in the PTRAK code are suited for droplets generated by a pressure atomizer where the gas phase flow field has little influence in the spray formation process. For the airblast atomizer (as used in the experimental set up) the spray formation process is found to be strongly influenced by the gas flow field, in particular, by the shear layer strength. Hence for realistic prediction of the trajectories and the evaporation characteristics, the droplet size class properties need to be characterized at the inlet which are in effect dictated by the gas flow field . For the PTRAK code, the droplet size classes at the inlet need to be characterized by their velocities and the injection angles. These parameters are more easily found for a pressure atomizer than an airblast atomizer where the spray formation process is independent of the gas flow velocities. Future research efforts should be directed towards estimating the initial conditions for the droplet size classes formed in an airblast atomizer for different flow conditions.

The modifications made to the PTRAK code has, however, improved its predictive capabilities significantly. A major deficiency of the ADD code is that the normal component of the mean gas phase velocity is set to zero everywhere in the flow domain. With the addition of the stochastic separated flow model, the effects of gas phase turbulence is considered in the droplet size class trajectory and evaporation characteristics calculations. This in effect introduces a non-zero normal component of the gas phase velocity in the droplet trajectory calculations. Computations are being carried out at Drexel to predict the spray evaporation charactersitics in a prevaporizing-premixing duct with the modified PTRAK code.

VI. REFERENCES

Anderson, O. L., Chiappetta, L. M., Edwards, D. E., Mcvey, J. B., 1982, "Analytical Modeling of Operating Characteristics of Premixing-Prevaporizing Fuel-Air Mixing Passage," Vol. 1.

Anderson, O. L. and Edwards, 1982, "Extensions to an Analysis of Turbulent Swirling Compressible Flows in Axisymmetric Ducts", NASA Contract NAS3-31853

Chen, K. Y., 1980, "Prediction of Channel and Boundary Layer Flows with a Low Reynolds Number Two Equation Model of Turbulence", AIAA-80-0134

Cox, E. R., 1923," Pressure Temperature Charts for Hydrocarbon Vapors", Industrial and Engineering Chemistry, Vol. 15, No. 6, pp. 592-593

Crowe, C.T., Sharma, M. P., Stock, D.E., 1977," The Particle-Source-ind-Cell (PSI-CELL) Model for Gas-Droplet Flows," J. Fluids Engineering, Vol. 99, pp. 325-332.

Dickerson, R. A. and Schuman, M. D, 1965,"Rate of Aerodynamic Atomization of Droplets", J. Spacecraft and Rockets, PP. 99-100

Dukowicz, J. K., 1980, J. Comp. Phys. 35, 229.

El Wakil, M. M., Uyehara, O. A. and Myers, P. S., 1954,"A Theoretical Investigation of the Heating Up Period of Injected Fuel Droplets Vaporizing in Air", NACA Tech. Note 3179

Farouk, B., Alber, W. B. and Mellor, A. M., 1987, "Spray Evaporation Studies in a Prevaporizing-Premixing Fuel Air Passage", 2nd ASME-JSME Thermal Engineering Joint Conference, Honolulu, Hawaii, Vol.1 , 159-164,

Farouk , B., Lau, W., Marakovits, S. and Mellor, A. M.,1987b, "Spray Evaporation Studies in a Confined Turbulent Shear Layer" ,The Combustion Institute (Eastern Section) Fall Technical Meeting, National Bureau of Standards, Gaithersburg, Maryland, 27-1 - 27-4,

Faeth, G. M., Shearer, A. J., Tamura, H., 1979," Evaluation of a Locally Homogeneous Flow Model of Spray Evaporation," J. of Energy, Vol. 3, pp. 271-278.

Feath, G. M., Mao, C.P., Szekely, G.A., Jr., 1980," Evaluation of a Locally Homogeneous Flow Model of Spray Combustion," J. of Energy, Vol. 4, pp, 78-87.

Faeth, G. M., 1983, "Evaporation and Combustion of Sprays," Prog. in Energy and Combustion Science, Vol. 9, pp. 1-76.

Gibson, M. M., Spalding, D. B. and Zinzer, W.,1970, Boundary Layer Calculations Using the Hassid-Poreh One Equation Energy Model", Letter in J. Heat and Mass Transfer, Vol.5, No.2, p.73

Gosman, A.D. and Ioannides, E., 1981, "Aspects of Computer Simulation of Liquid-Fuel Combustors," AIAA Paper No. 81-0323.

Grinstein, F. F., Oran, E. S. and Boris, J. P., 1986, "Numerical Simulations of Asymmetric Mixing in Planar Shear Flows", J. Fluid Mech., Vol.165, p. 201

Hetchkiss, R. S. and Hirt, C. W., 1972, "Particulate Transport in Highly Distorted Three-Dimensional Flow Field" Los Alamos Scientific Laboratory Preprint LA-DC-72-364.

Hirschfelder, J.O, Curtiss, C. F. and Bird, R. B., 1954,"Molecular Theory of Gases and Liquids", Wiley

Hinze, J. O., 1975, "Turbulence," McGraw-Hill, New York, pp. 427-428.

Jurewica, J. T., and Stock, D. E., 1976, "A Numerical Model for Turbulent Diffusion in Gas-Particle Flows," ASME Paper No. 76-WA/FE-33.

Jones, W. P. and Launder, B. E., 1972," The Prediction of Laminarization with a Two Equation Model of Turbulence", Int. J. Heat Mass Transfer, Vol. 15, pp. 301-314

Keller, H. B., 1970, "A New Difference Scheme for Parabolic Problems, Numerical Solution of Partial Differential Equations" II SYNSPADE , Academic Press, New York

Keller H. B., 1968, "Accurate Difference Methods for Linear Ordinary Differential Systems Subject to Linear Constraints", SIAM J. Numerical Analysis, Vol. 6, No.1

Launder, B. E., Pridden, C. H. and Sharma, B. I., 1977, "The Calculations of Turbulent Boundary Layers on Spinning and Curved Surfaces", Trans. ASME J. Fluids Eng., p.231

Mellor, A. M., 1980, "Semi-empirical Correlations for Gas Turbine Emissions, Ignition and Flame Stabilization", Prog. Energy Combust. Sci., vol. 6, pp. 347-358

Panaik, G. , 1986, " A Numerical Simulation of Droplet Vaporization with Convection", Ph. D Thesis, Carnegie-Mellon University, Pittsburgh, Pa.

Priem, R. J. and Heidmann, M. F., 1960,"Propellent Vaporization as a Design Criteria for Rocket -Engine Combustion Chambers", NASA Tech Report, R-67.

Shuen, J. S., 1984, "A Theoretical and Experifmental Investigation of Dilute Particle-Laden Turbulent Gas Jets," Ph.D. Thesis, The Pennsylvania State University.

Simmons, H. C, 1977, " The Correlation of Drop Size distribution in Fuel Nozzle Sprays", J. Eng. Power, Vol. 99, No. 3, 309 - 319

Sonin, A. A., 1983, "Calibration of the k - ε Turbulence Model for the Diffusion of Turbulence", Physics of Fluids, Vol. 26, p.2769

Varah, J. M., 1972, "On the Solution of Block Tridiagonal Systems Arising from Certain Finite Difference Equations", Mathematics of Computations, Vol. 26, No. 120

APPENDICES

I. List of all publications under sponsorship of ARO
(Contract No. DAAL03 -87 - K 0015)

II. List of all participating scientific personnel

I. List of all publications under sponsorship of ARO

(Contract No. DAAL03 -87 - K 0015)

1. "Spray Evaporation Studies in a Prevaporizing-Premixing Fuel Air Passage", B. Farouk, W. B. Alber and A. M. Mellor, 2nd ASME-JSME Thermal Engineering Joint Conference, Honolulu, Hawaii, Vol.1 , 159-164, March 1987.

2. "Spray Evaporation Studies in a Confined Turbulent Shear Layer" , B. Farouk , W. Lau, S. Marakovits and A. M. Mellor, The Combustion Institute (Eastern Section) Fall Technical Meeting, National Bureau of Standards, Gaithersburg, Maryland, 27-1 - 27-4, November 2-6, 1987

3. " Dispersion Effects on Droplets in a Prevaporizing-Premixing Fuel Air Passage", B. Farouk, X. X. Cai and A. M. Mellor, National Heat Transfer Conference, Philadelphia, Pa., August, 1989 (submitted)